Roles of URLs in Probing Controls on Induced Seismicity and Related Permeability Evolution

Derek Elsworth (Penn State), Chris Marone (PSU), Josh Taron (USGS),
Ghazal Izadi (GMI/BH), Quan Gan (PSU), Zhen Zhong (PSU), Yi Fang (PSU), Thibault Candella (BH)

Hydraulic Fracturing
- Gas Fracturing
- Unknowns
- Field Experiments

EGS/CO2 Sequestration
- Key Questions
- Field Experiments
- Geodetic and Downhole Measurements

Summary

Key Coupled Processes Related to Gas-Fracturing in Unconventional Reservoirs

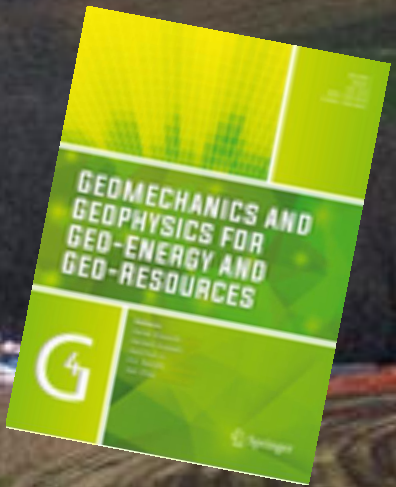

Derek Elsworth, Quan Gan, Chris Marone, Peter Connolly[1], Jenn Alpern, Yinlong Lu[2], Brian Culp and Kyungjae Im, Jiehao Wang[2], Wancheng Zhu[3], Jishan Liu[4], Yves Guglielmi[5], Xiang Li, Zijun Feng

Center for Geomechanics, Geofluids, and Geohazards (G3)
Energy and Mineral Engineering, Geosciences and EMS Energy Institute The Pennsylvania State University

and [1]Chevron ETC, [2]CUMT-X, [3]NEU, [4]CAS/UWA, [5]Aix-Marseille

Motivation

Gas Recovery (Improved production)

- Energetic fracturing – reducing diffusion lengths

Incidental Benefits (Improved environmental protection)

- Decrease water usage
  - Resource usage
  - Induced seismicity
  - Reduce surface transportation/disruption
- Minimize effect on sensitive reservoir rocks
  - Avoid pore occlusion with fluids
  - Avoid swelling of clays
  - Avoid recovery of NORMS
- Reduce life-cycle equivalent CO_2 costs

Fluid Delivery

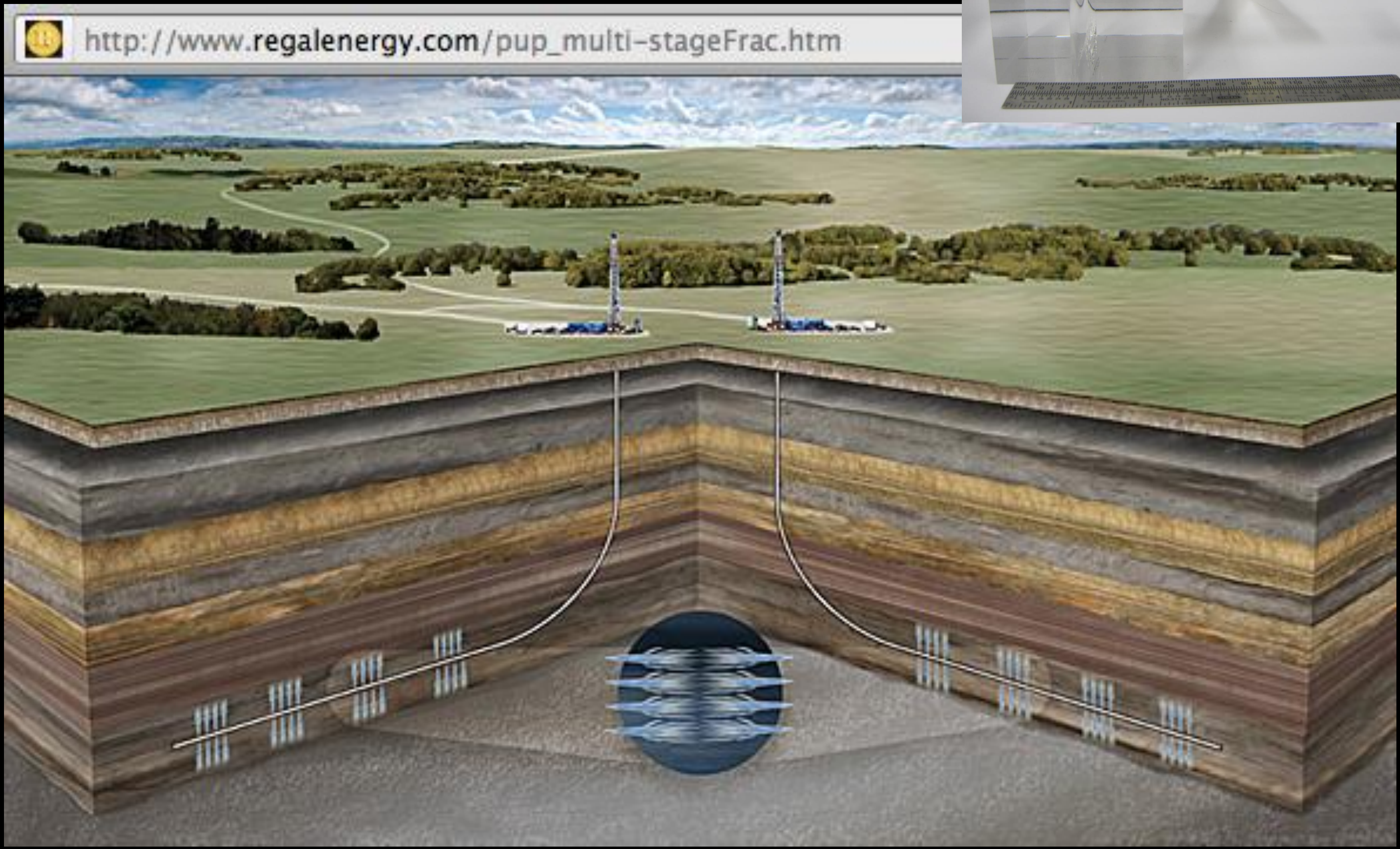

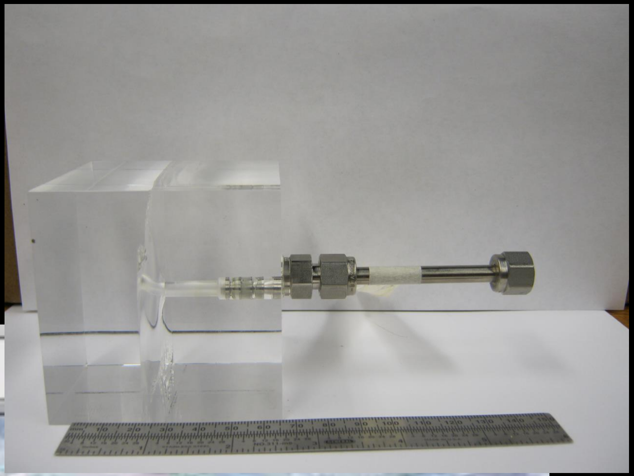

Borehole Fracture in PMMA (Polymethyl methacrylate aka: Lucite, Plexiglas, Perspex, Acrylic)

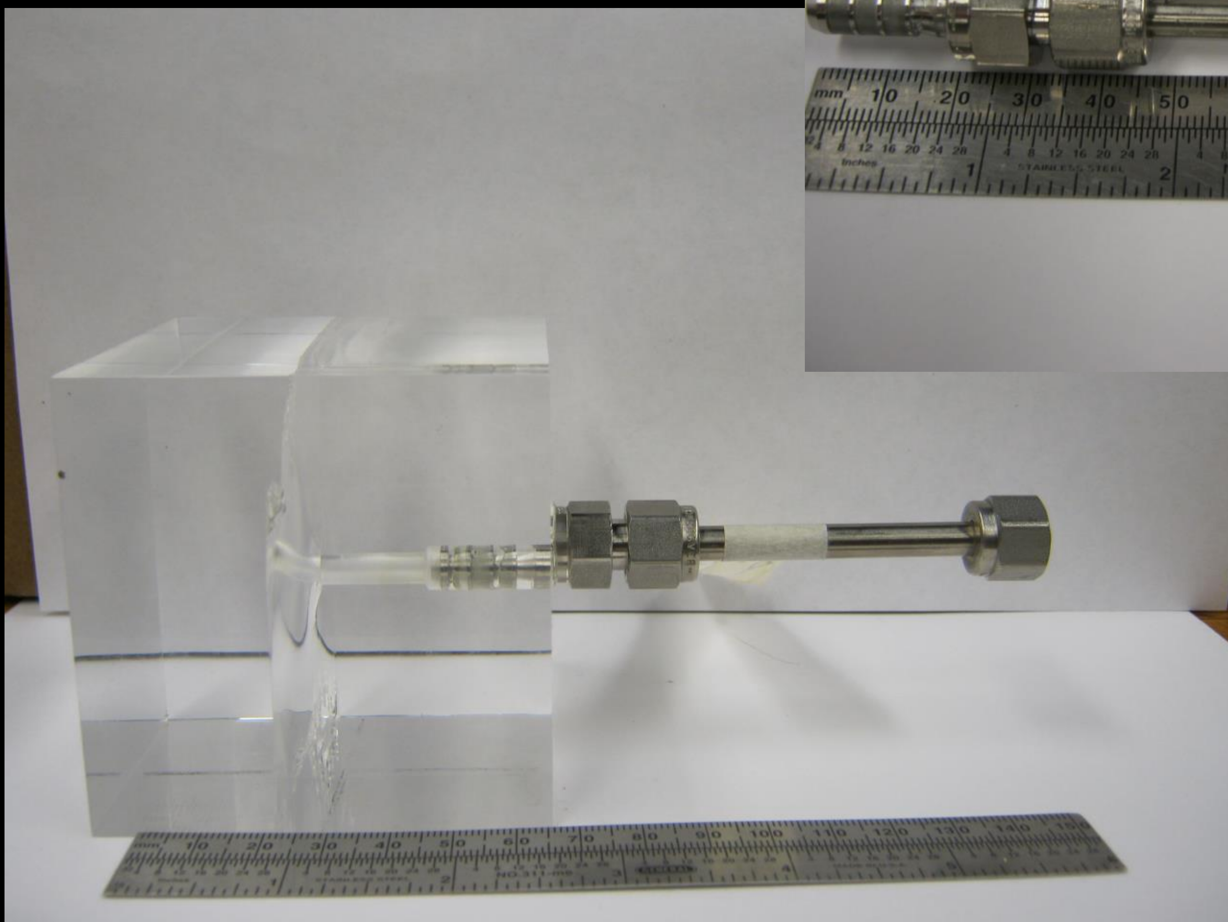

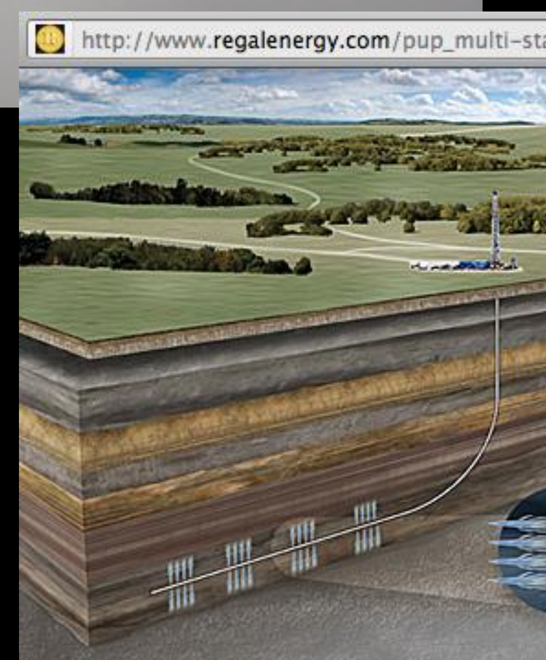

Stress State

$$\sigma_1 > \sigma_2 > \sigma_3$$

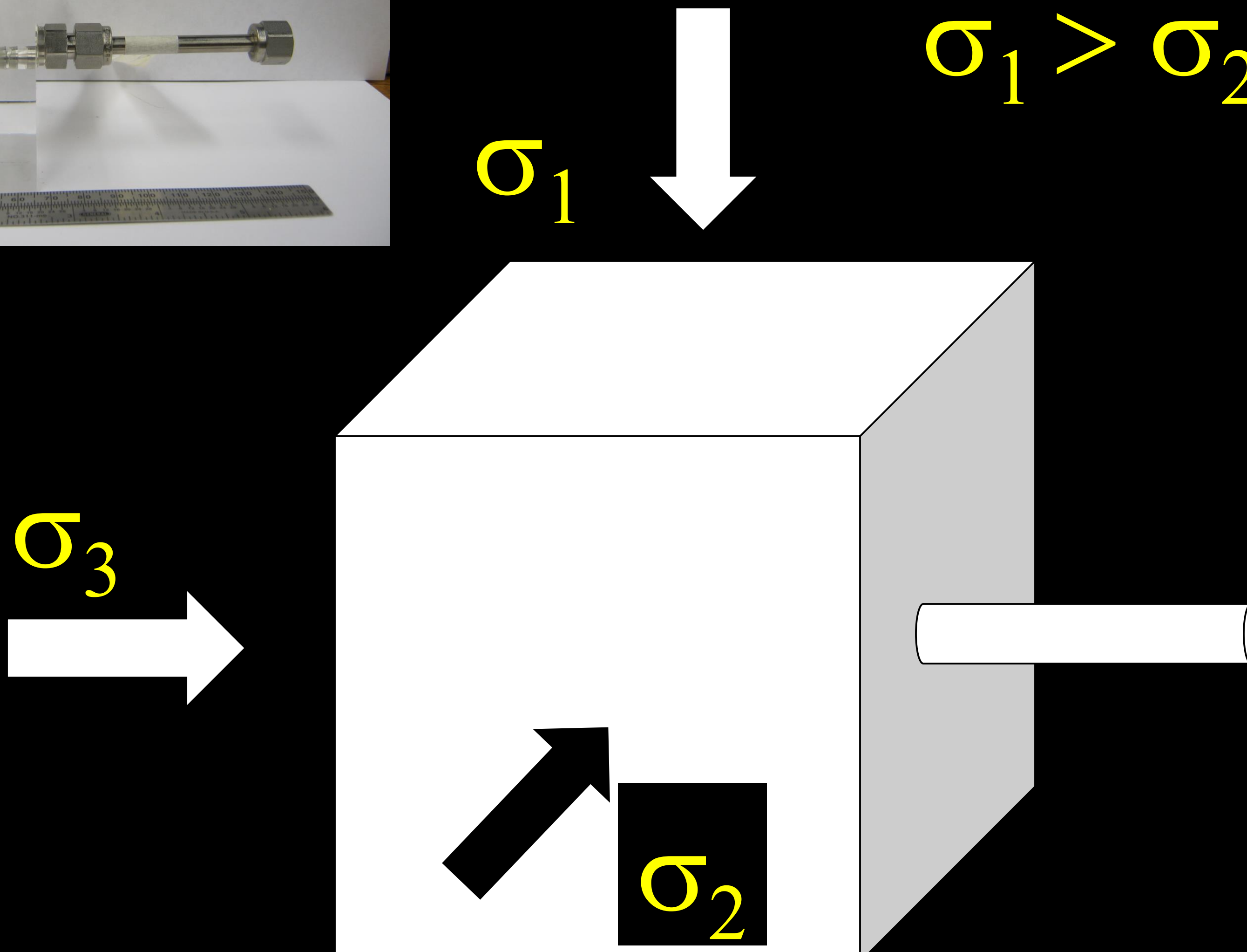

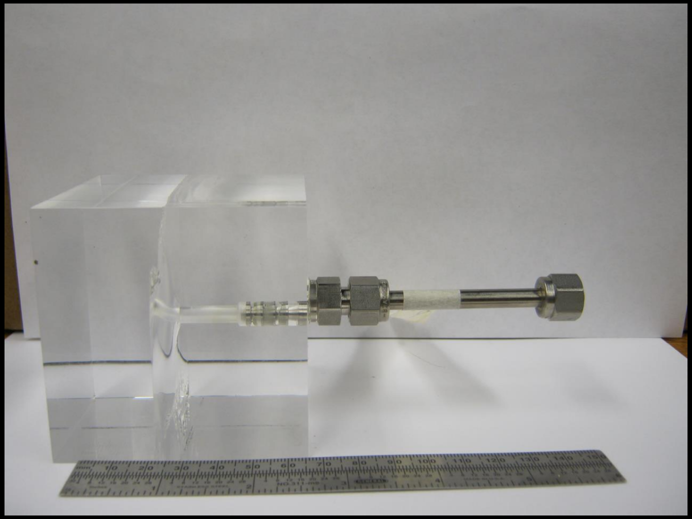

Hydrofracture, view below is in the σ_3 direction

$\sigma_1 = \sigma_2$ = 10 MPa (≈1500 psi)
Pp fail = 43.3 MPa (≈ 6200 psi)

p3006; water

PMMA: N_2 hydrofrac

PMMA:

N_2 hydrofrac

H_2O hydrofrac

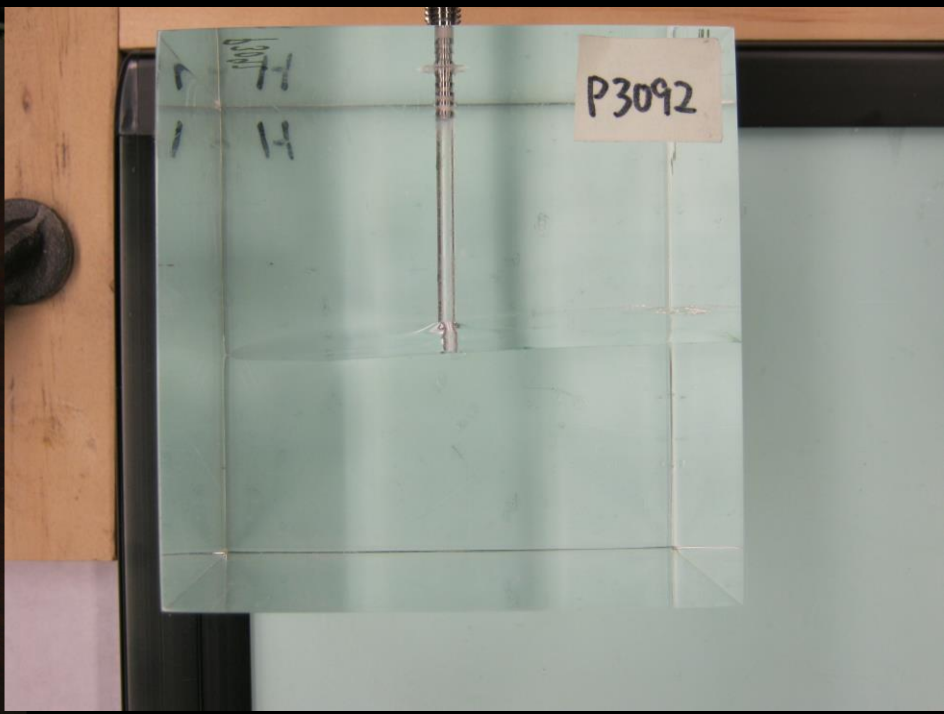

P_b is fluid/fluid-state dependent

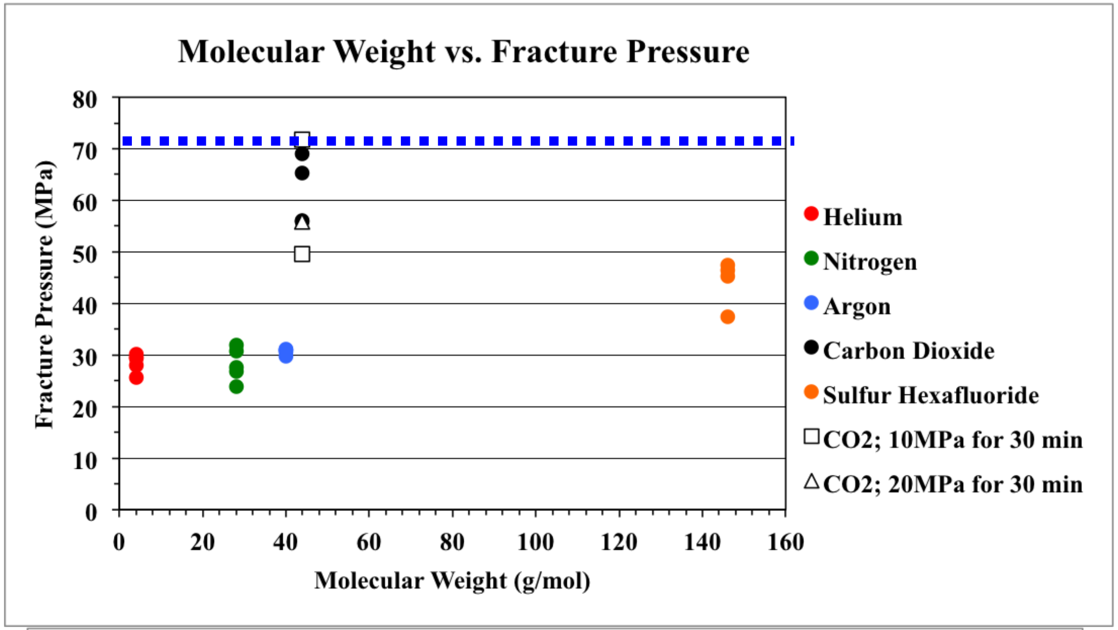

S_h=S_v=5 MPa

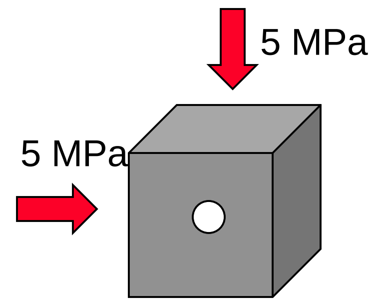

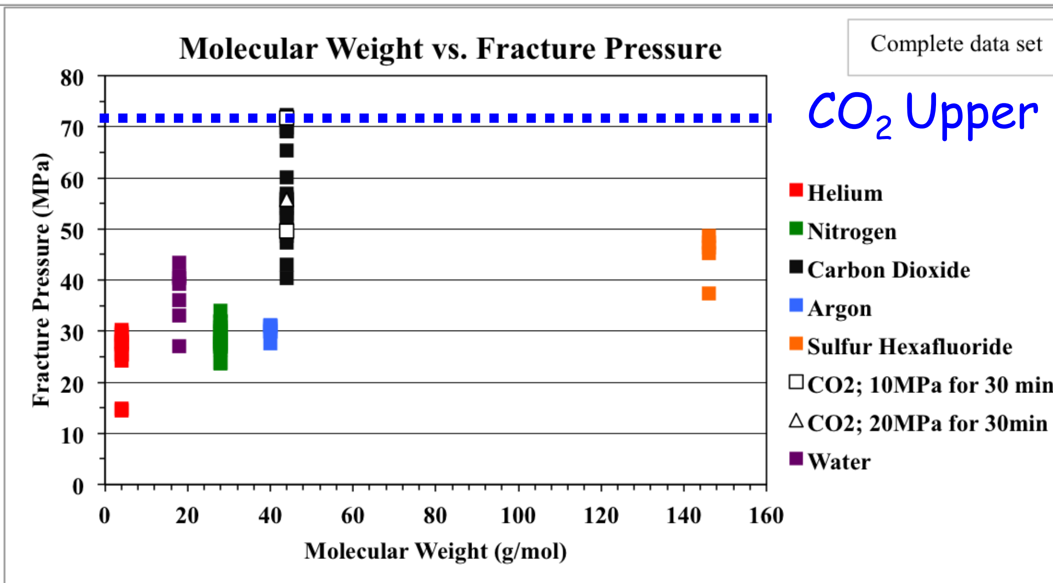

CO_2 Upper Bound - Tensile Strength ~ 70 MPa

All Data

P_b for CO_2:N_2 are ~2:1 for PMMA/Bluestone

PMMA

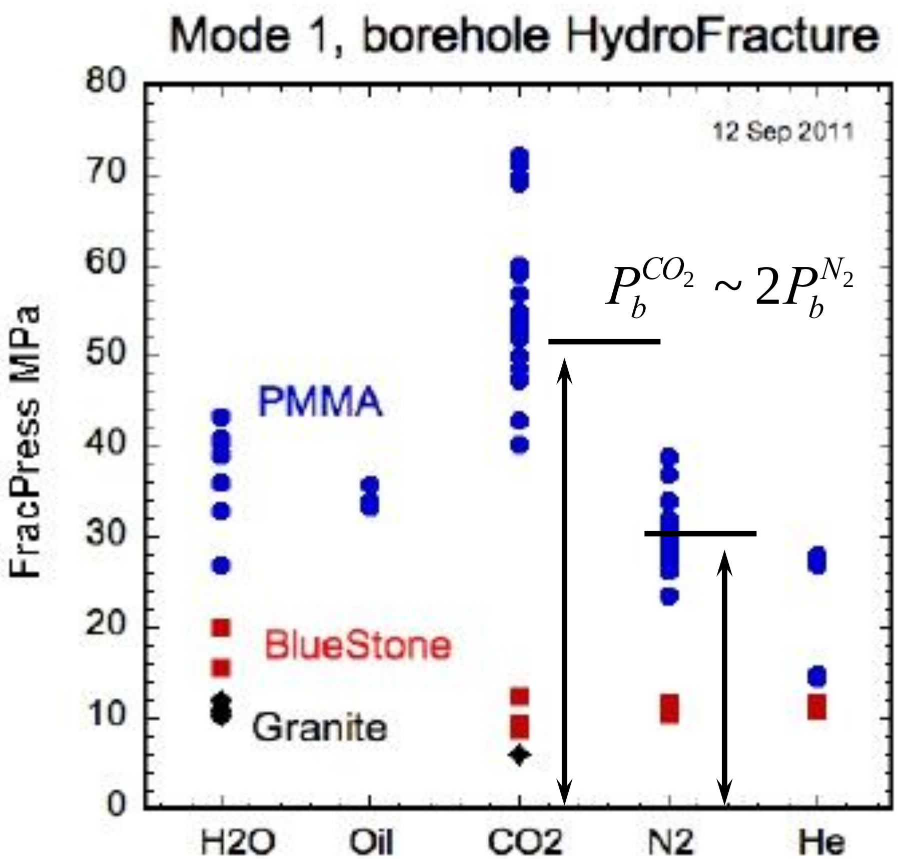

Rock

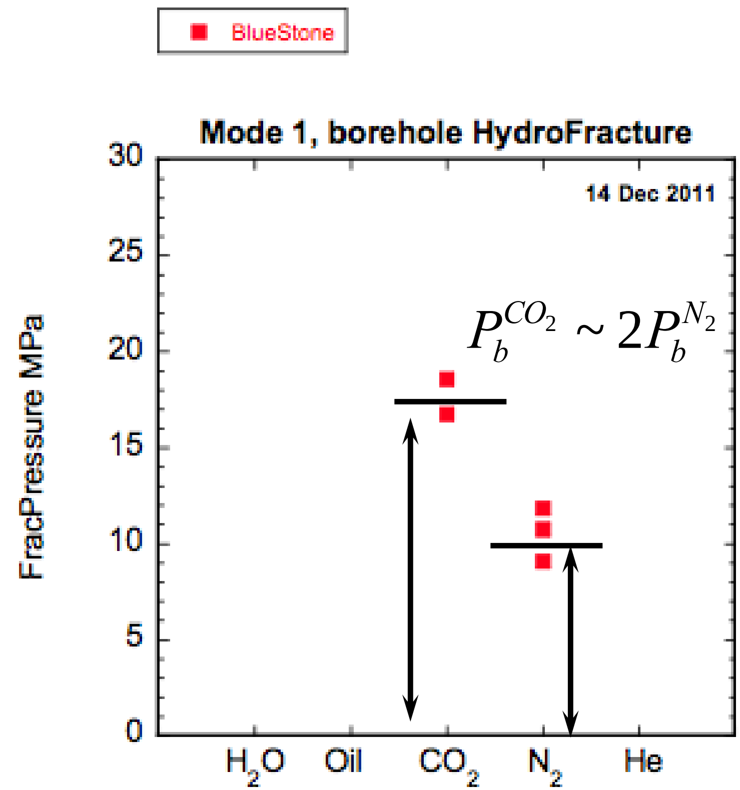

Fracturing Fluid Properties

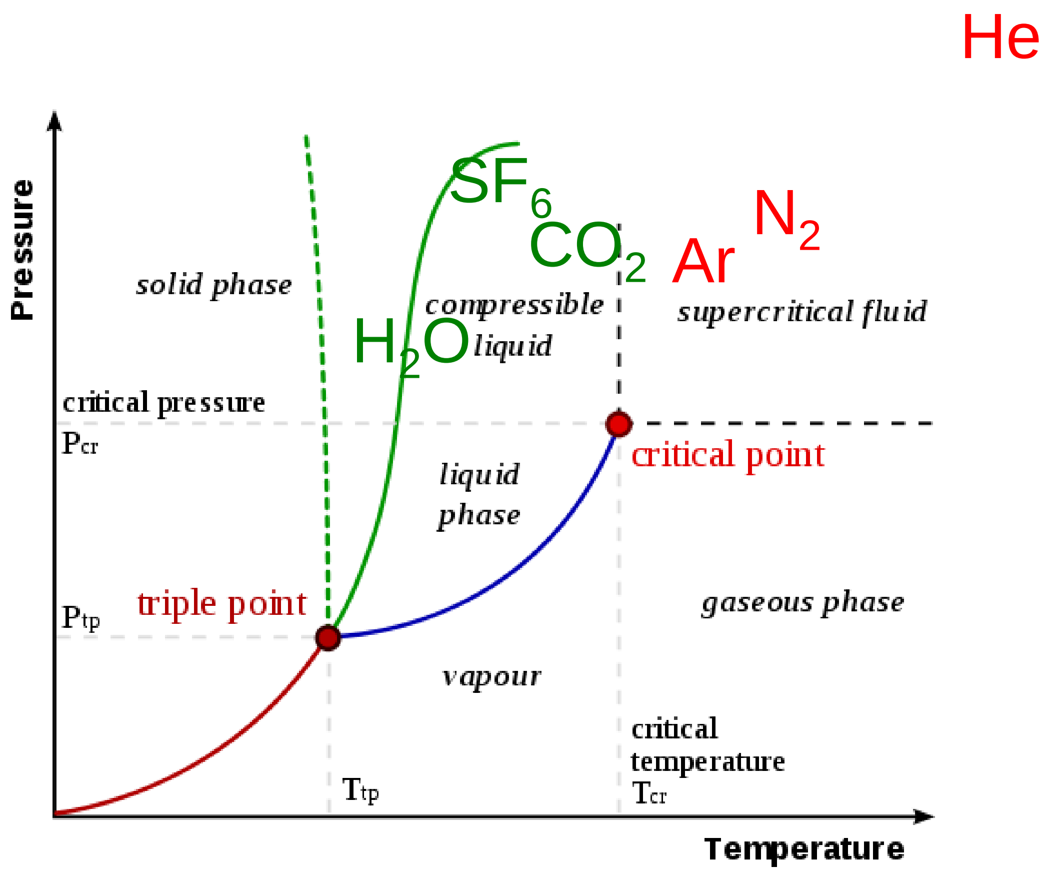

Substance[3][4]	Critical temperature	Critical pressure (absolute)
Helium	−267.96 °C (5.19 K)	2.24 atm (227 kPa)
Hydrogen	−239.95 °C (33.20 K)	12.8 atm (1,300 kPa)
Neon	−228.75 °C (44.40 K)	27.2 atm (2,760 kPa)
CH_4 (Methane)	−82.3 °C (190.9 K)	45.79 atm (4,640 kPa)
Nitrogen	−146.9 °C (126.3 K)	33.5 atm (3,390 kPa)
Fluorine	−128.85 °C (144.30 K)	51.5 atm (5,220 kPa)
Argon	−122.4 °C (150.8 K)	48.1 atm (4,870 kPa)
Oxygen	−118.6 °C (154.6 K)	49.8 atm (5,050 kPa)
Krypton	−63.8 °C (209.4 K)	54.3 atm (5,500 kPa)
Xenon	16.6 °C (289.8 K)	57.6 atm (5,840 kPa)
CO_2	31.04 °C (304.19 K)	72.8 atm (7,380 kPa)
N_2O	36.4 °C (309.6 K)	71.5 atm (7,240 kPa)
Ammonia[5]	132.4 °C (405.6 K)	111.3 atm (11,280 kPa)
Chlorine	143.8 °C (417.0 K)	76.0 atm (7,700 kPa)
Bromine	310.8 °C (584.0 K)	102 atm (10,300 kPa)
Water[6][7]	373.946 °C (647.096 K)	217.7 atm (22,060 kPa)
H_2SO_4	654 °C (927 K)	45.4 atm (4,600 kPa)
Sulfur	1,040.85 °C (1,314.00 K)	207 atm (21,000 kPa)
Mercury	1,476.9 °C (1,750.1 K)	1,720 atm (174,000 kPa)
Caesium	1,664.85 °C (1,938.00 K)	94 atm (9,500 kPa)
Ethanol	241 °C (514 K)	62.18 atm (63 bar, 6,300 kPa)
Lithium	2,950 °C (3,220 K)	652 atm (66,100 kPa)
Gold	6,977 °C (7,250 K)	5,000 atm (510,000 kPa)
Aluminium	7,577 °C (7,850 K)	
Iron	8,227 °C (8,500 K)	

1. Ar, N_2 and He are supercritical (no interfacial tension)
2. Water, CO_2 and SF_6 are liquids (interfacial tension)

SF_6 [46C; 3.6MPa]

[Source: http://en.wikipedia.org/wiki/Critical_point_(thermodynamics)]

Fracture Complexity

Super-critical Fluids

Helium, He

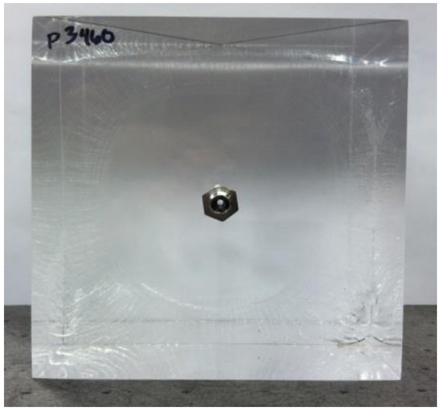

Nitrogen, N_2

Argon, Ar

Sub-critical Fluids

Carbon Dioxide, CO_2

Water, H_2O

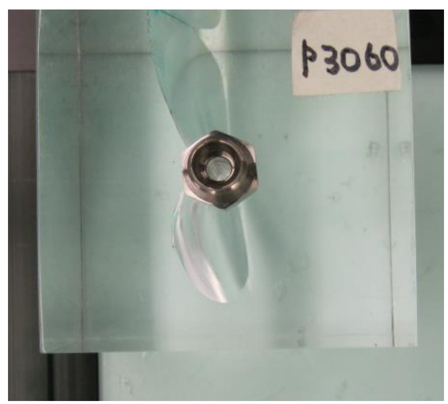

Sulfur Hexafluoride, SF_6

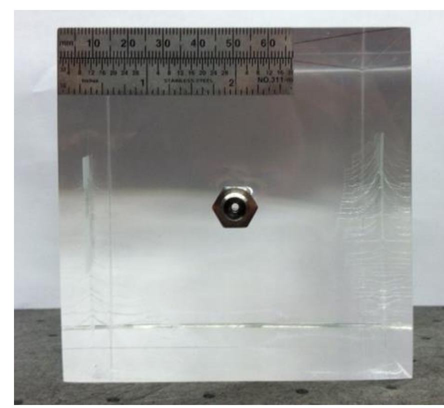

Fracture / Complexity

Fracture Complexity

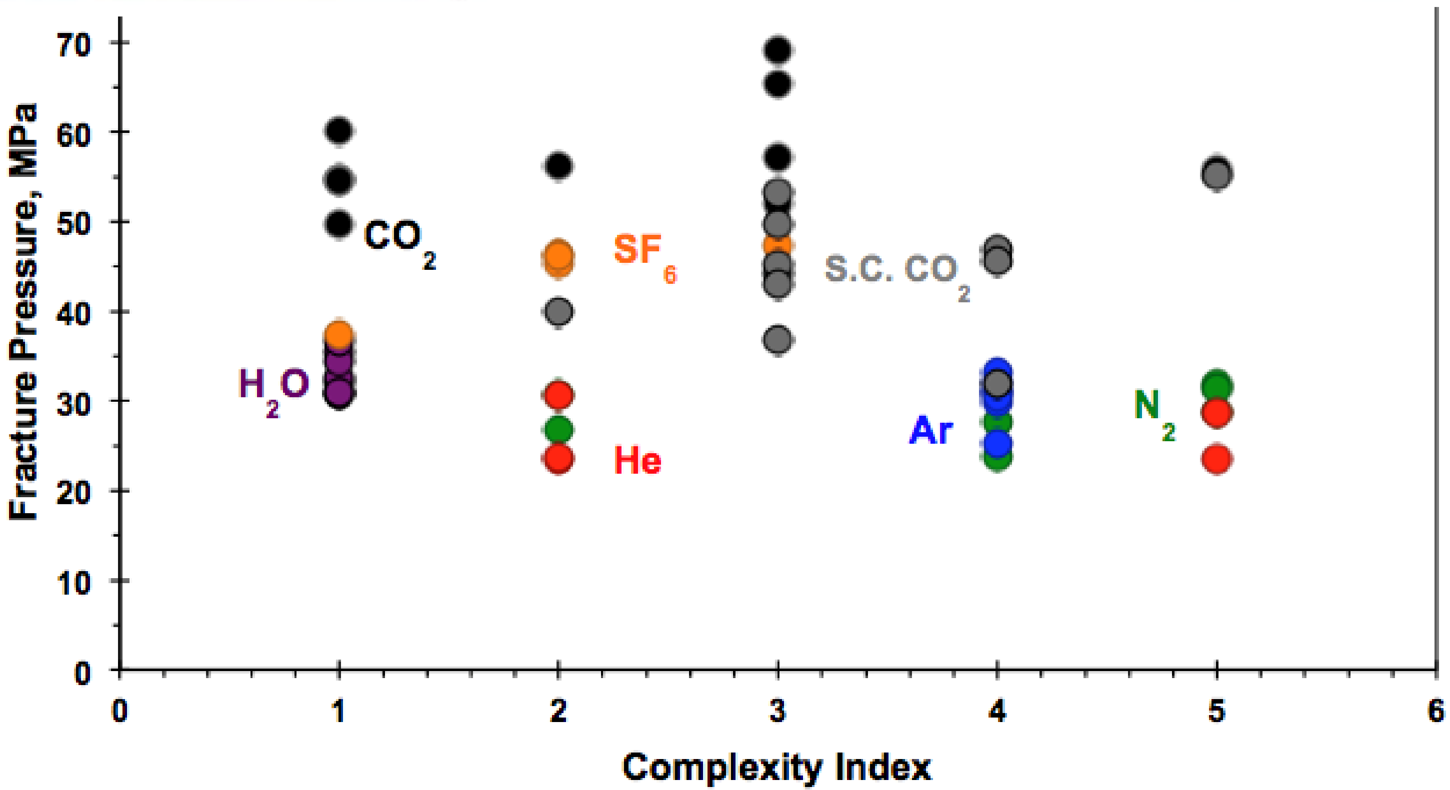

PMMA

Longitudinal Hydraulic Fracture

Fracture Breakdown Pressure for fracture along borehole (plane strain)

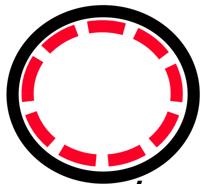

"Permeable:" $\sigma_T = \sigma_{\theta\theta} = 3S_h - S_H - P_0 + (1+\eta)P_w$

$$\eta = \frac{\nu}{1-\nu}\alpha \; therefore \; \eta[0 \rightarrow \alpha]$$

$$P_w = \frac{\sigma_T - 3S_h + S_H + P_0}{(1+\eta)}$$

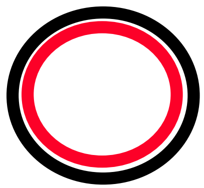

"Impermeable:" $\sigma_T = \sigma_{\theta\theta} = 3S_h - S_H - P_0 + P_w$

$$P_w = \sigma_T - 3S_h + S_H + P_0$$

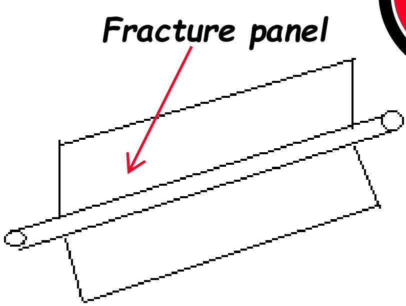

$PMMA : \nu = 0.36; \alpha = 1?$

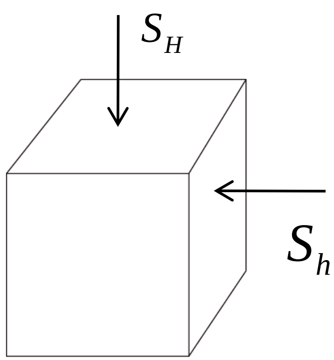

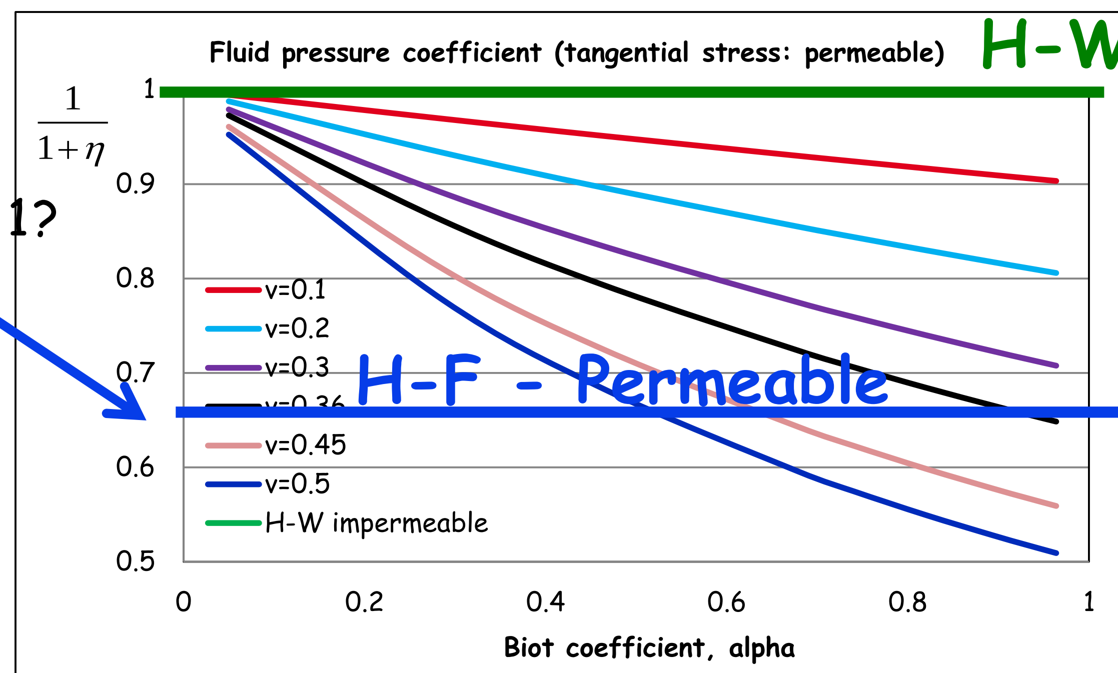

Entry Pressures into Borehole Wall

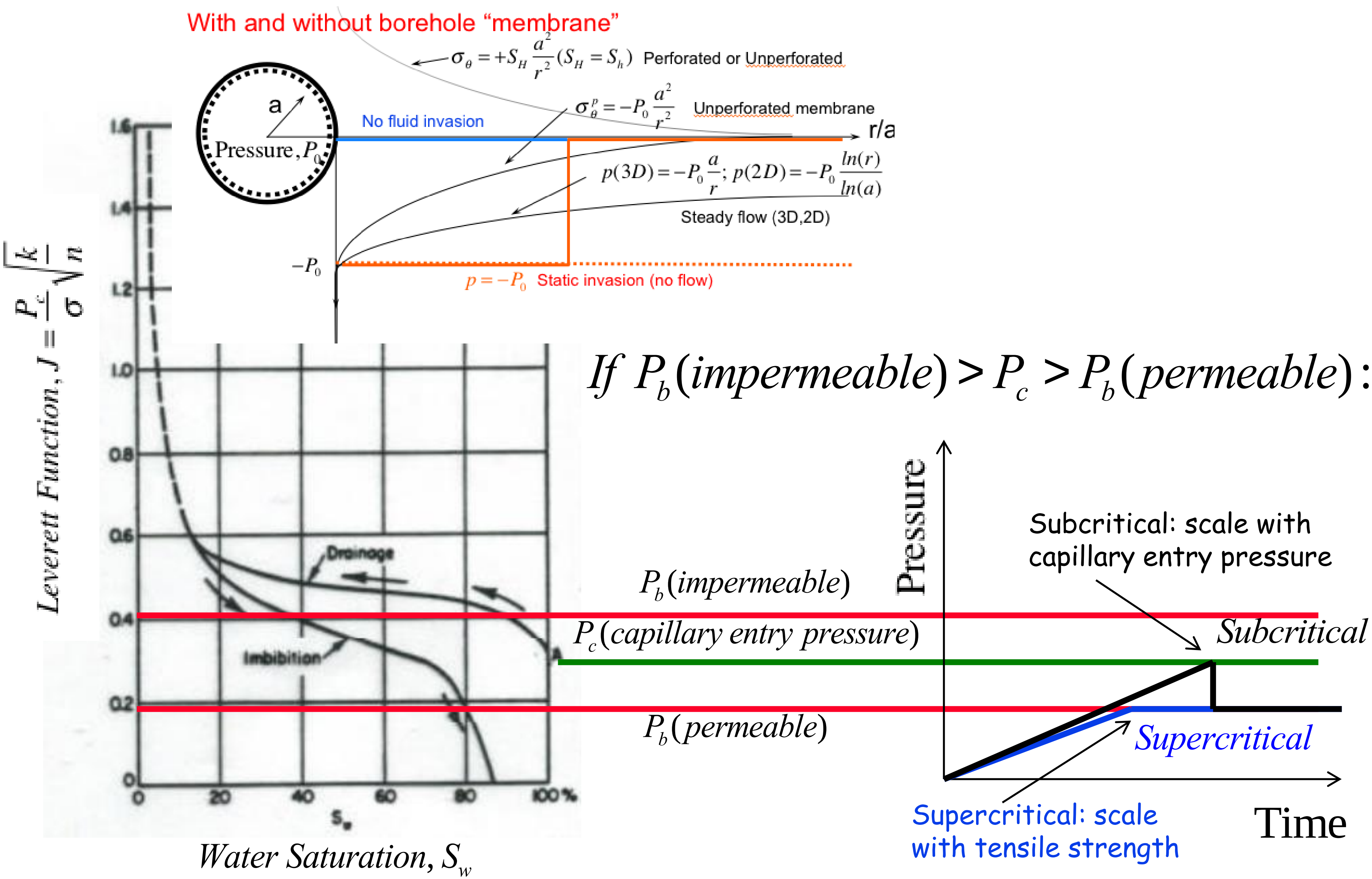

Fluid Invasion - SubCrit/SuperCrit

Quantify breakdown pressure relationship with interfacial tension

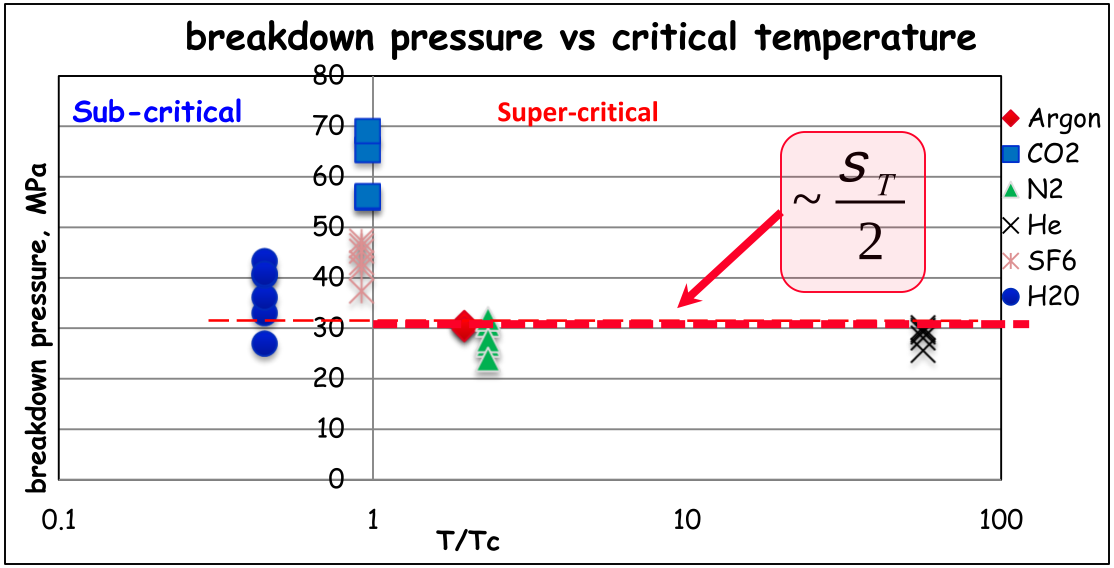

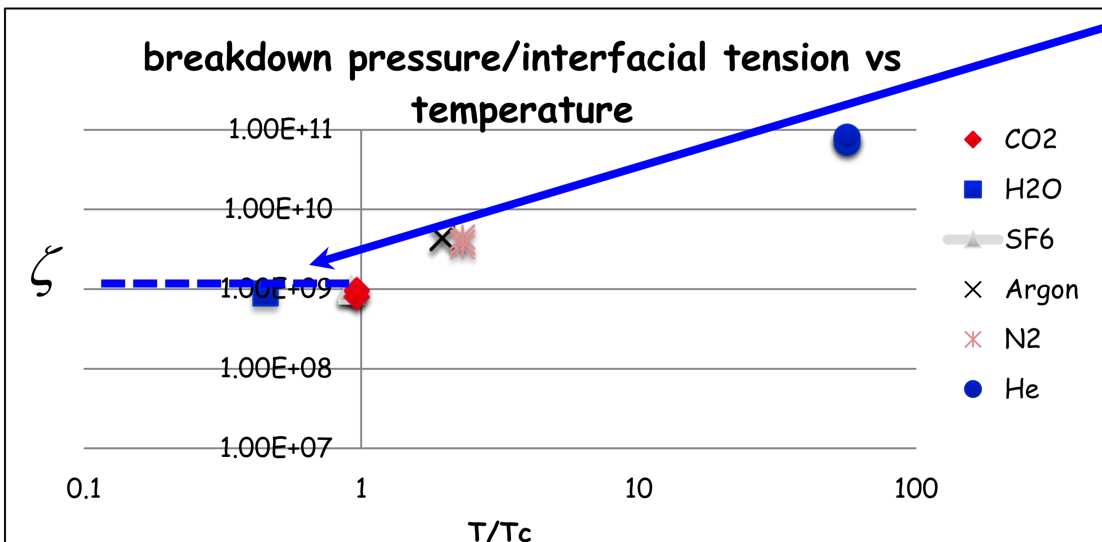

Super-critical (invasion):

1. Pb dependent on tensile strength
2. Pb independent of interfacial tension

Sub-critical (no-invasion):

Invasion pressure scales with, J :

$$J = \frac{P_c}{s}\sqrt{\frac{k}{n}}$$

$$V = \frac{P_b}{s} = \frac{MPa}{mN/m} = \frac{10^6 N/m^2}{10^{-3} N/m} = \frac{10^9}{m}$$

Therfore:

1. Pb independent of tensile strength
2. Pb dependent on interfacial tension

Modeling – Damage Mechanics

Microscopic-macroscopic model

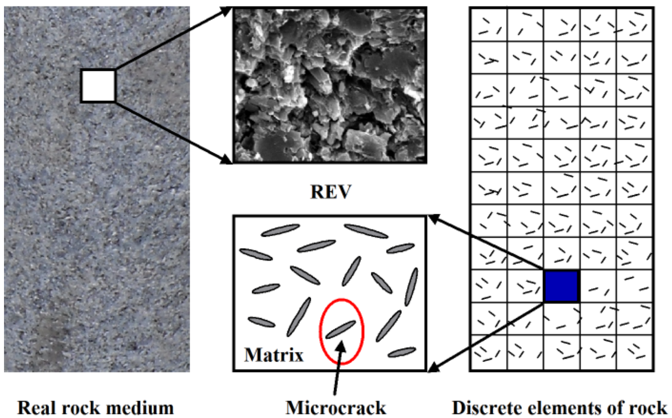

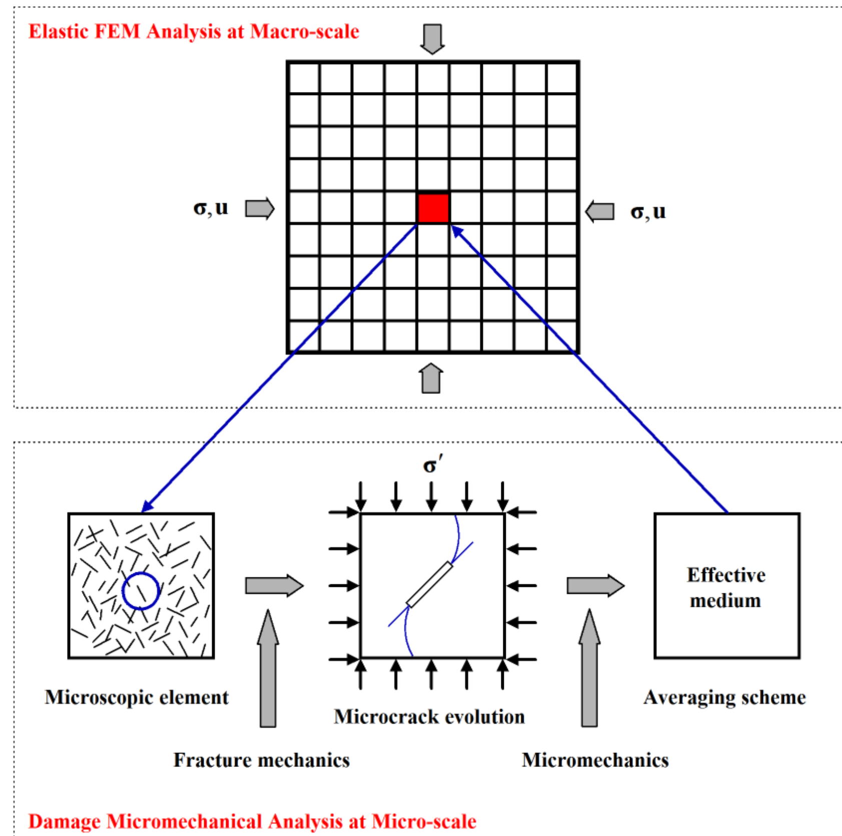

Specimen geometry

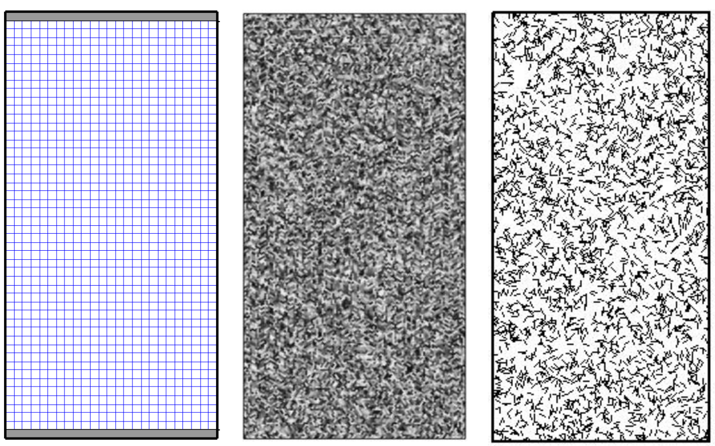

[Lu et al., Computers and Geotechnics, 2013]

Water fracturing vs. gas fracturing

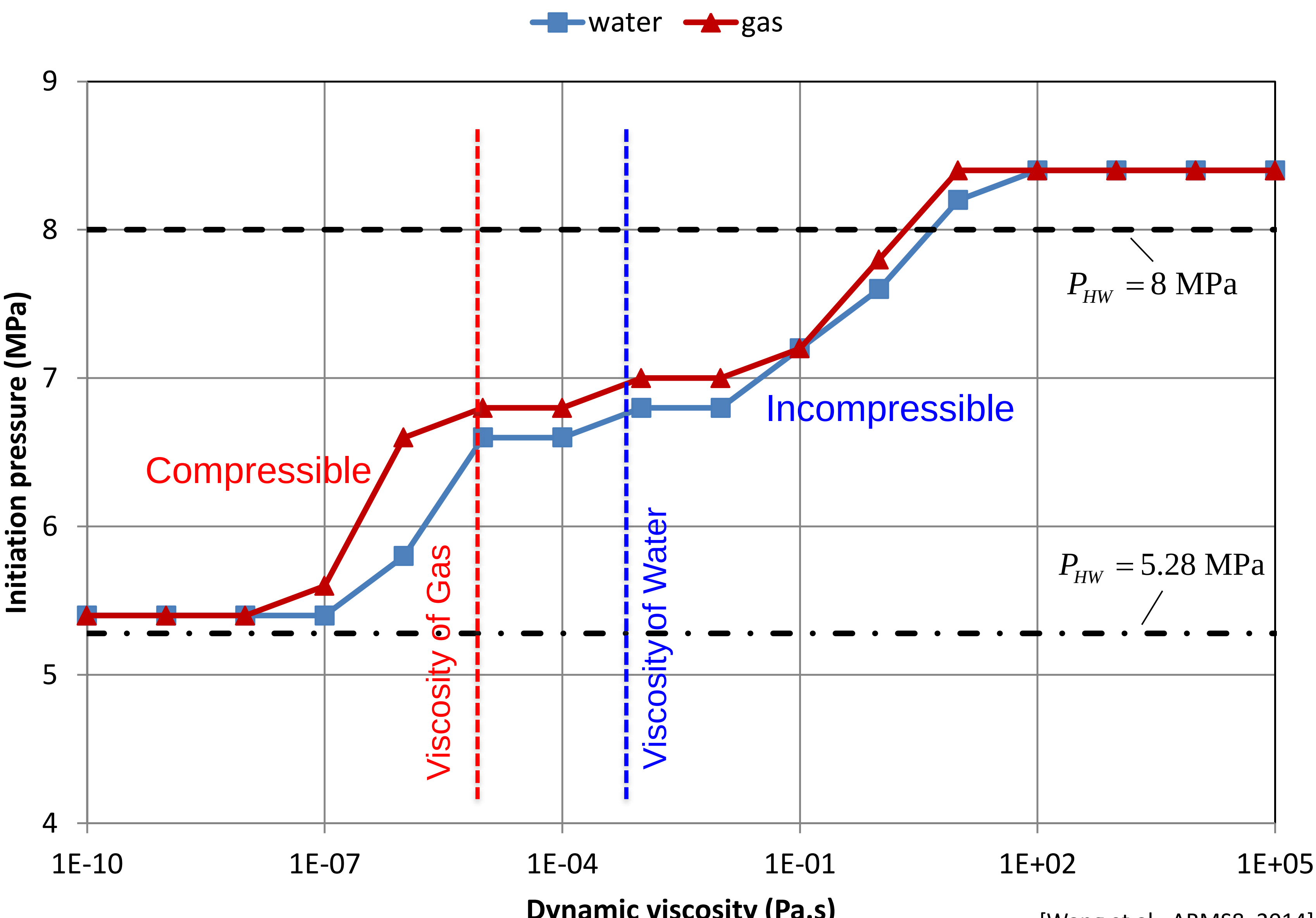

[Wang et al., ARMS8, 2014]

Modeling – Fracture Propagation

Driven by fluid pressure

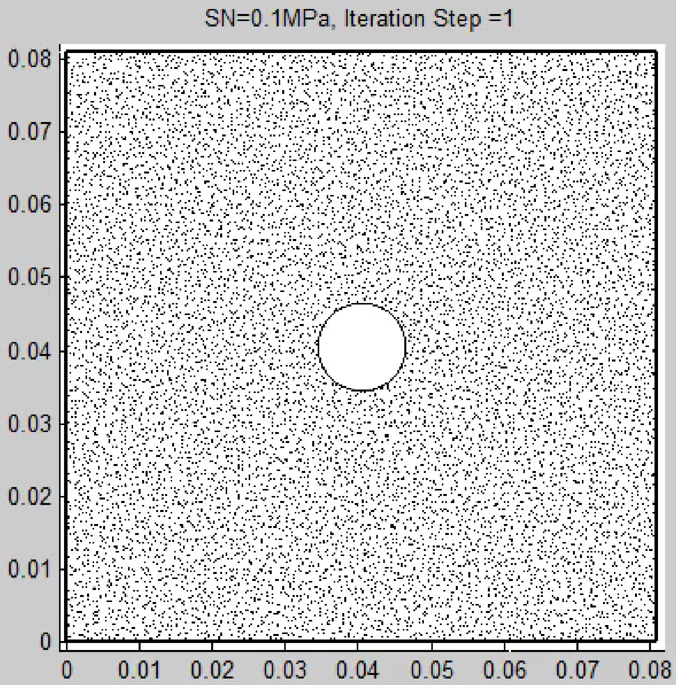

Microcrack growth

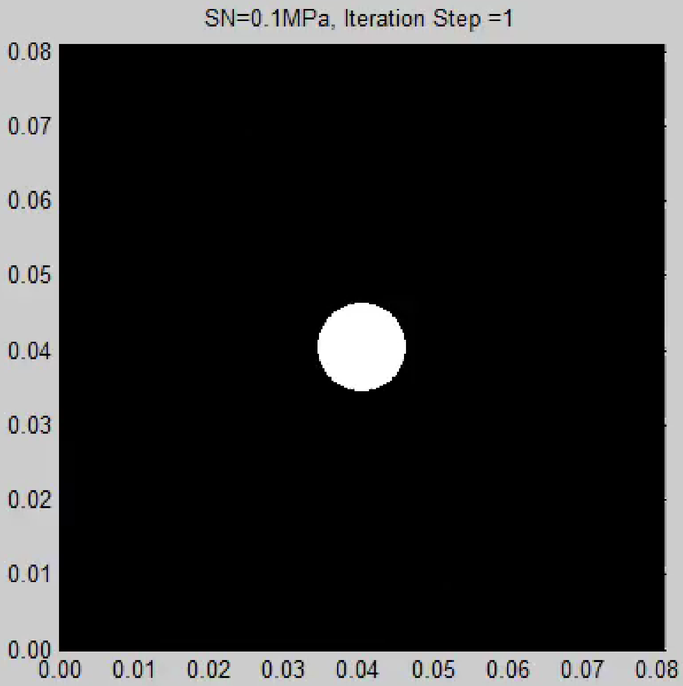

Macrocrack growth

Modeling - Hydraulic fracturing with ideal gas

Confining stress ratio of 6:1 | Confining stress ratio of 1:1

Gas fracturing (Compressible)

with the same material parameters of rock and pressurization rate

Water fracturing (Incompressible)

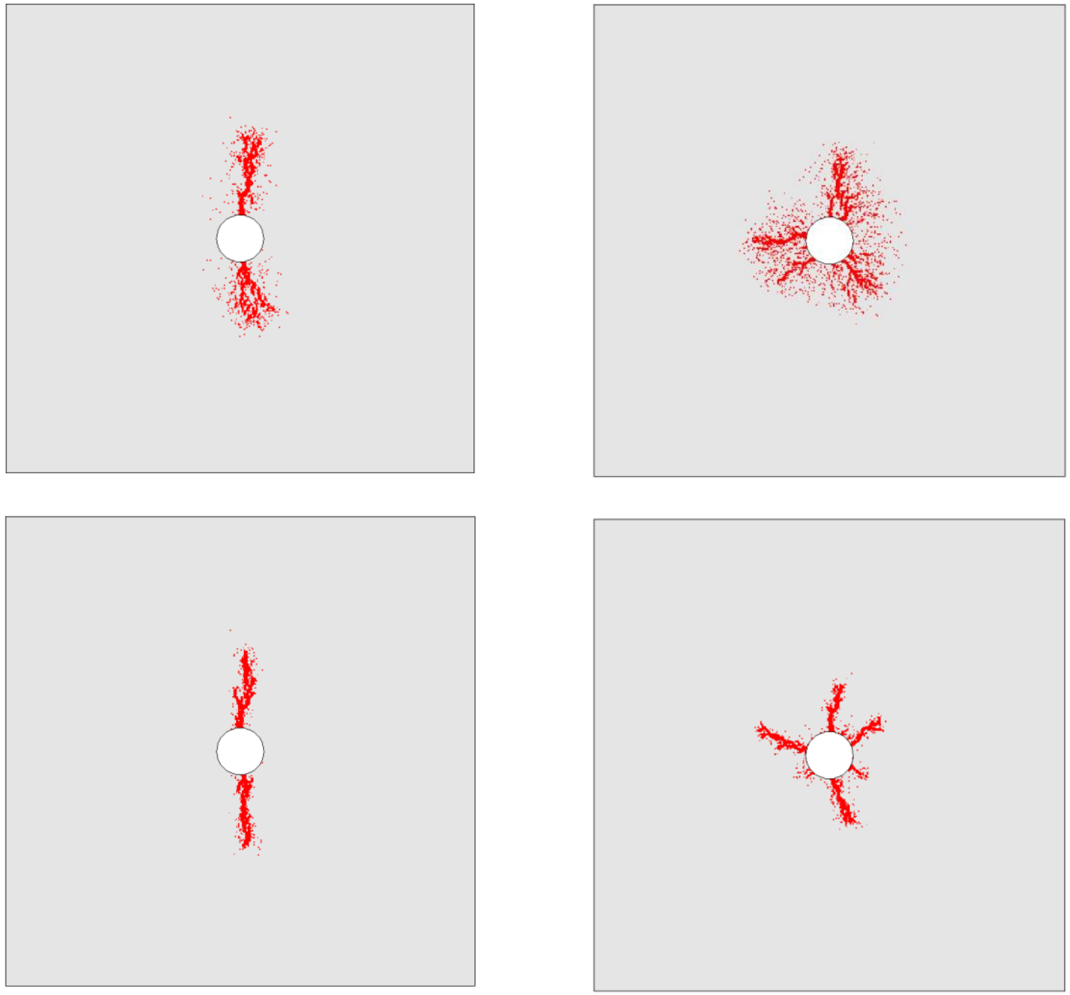

Experimental concept and layout

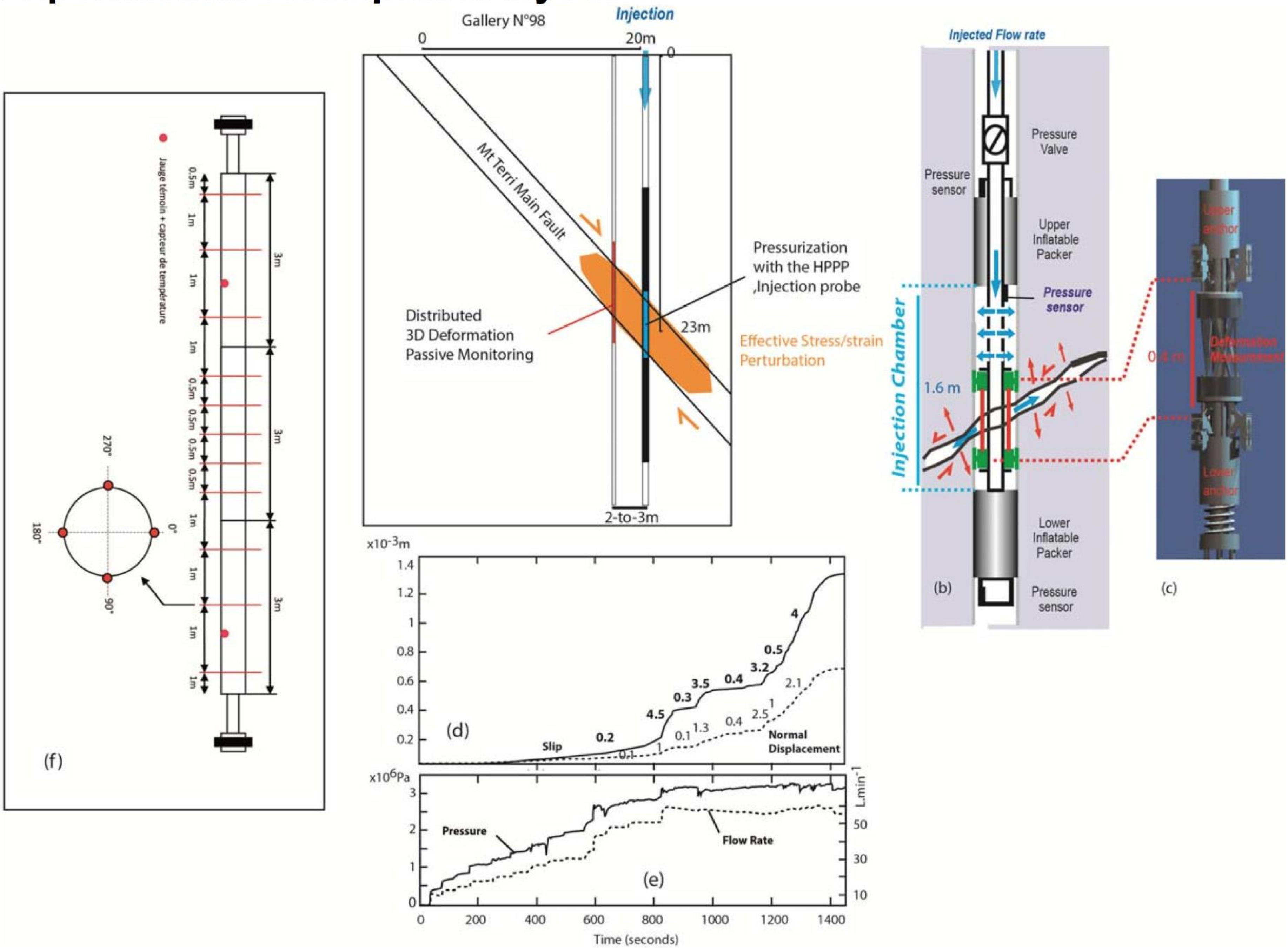

In Situ Experimentation – Gas Fracturing

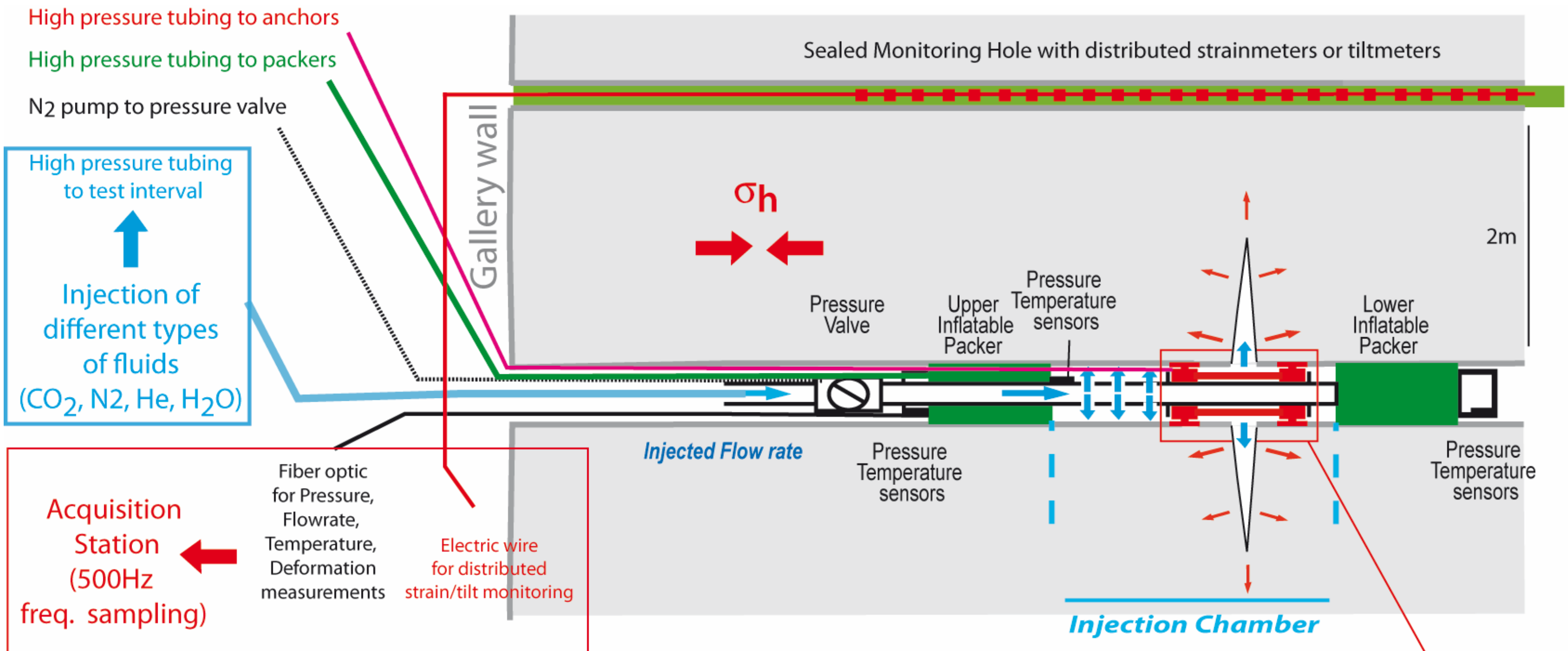

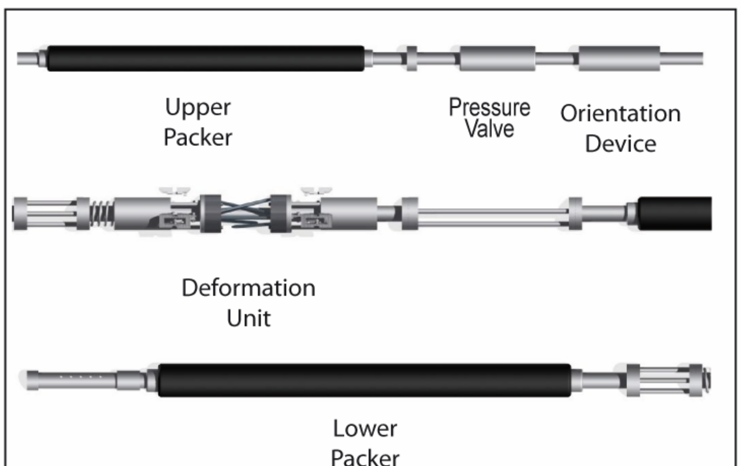

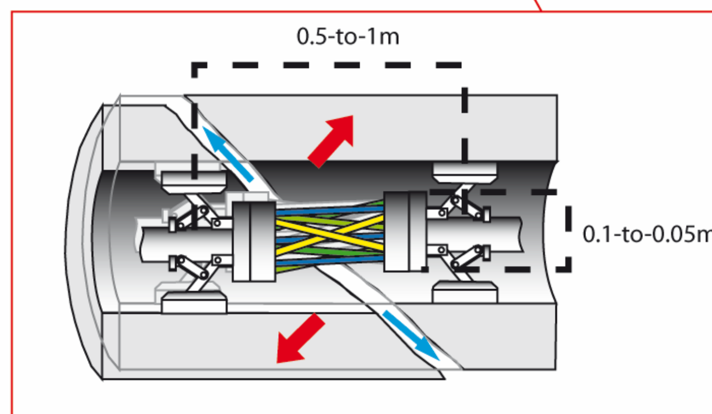

3D Monitoring of the Hydraulic Fracture propagation


Ga04
Ga08

Summary

Shale gas is a significant resource and offers:

- Energy: Security, Independence and Environment
- Has a variety of water-related issues
- Waterless fracturing offers some advantages if understood

Advantages of gas fracturing

- Reduced water use
- Potential sequestration if GHG
- Generation of complex fracture networks
- Enhanced Shale Gas Recovery if CO_2

Experiments indicate some promise with behavior related to:

- Breakdown pressures related to gas state/type
- Fracture complexity related to gas state/type
  - Supercritical N_2 more complex, He less complex… why?

Improved mechanistic understanding needed to fully utilize the promise of these observations

- Integrated program across scales – Observation – Expt. - Analysis
- Determine benefits:
  - Feasibility/productivity/longevity
  - Environment: Water consumption/protection and induced seismicity….

Roles of URLs in Probing Controls on Induced Seismicity and Related Permeability Evolution

Derek Elsworth (Penn State), Chris Marone (PSU), Josh Taron (USGS),
Ghazal Izadi (GMI/BH), Quan Gan (PSU), Zhen Zhong (PSU), Yi Fang (PSU), Thibault Candella (BH)

Hydraulic Fracturing

- Gas Fracturing
- Unknowns
- Field Experiments

EGS/CO2 Sequestration

- Key Questions
- Field Experiments
- Geodetic and Downhole Measurements

Summary

Key Questions in SGRs and EGS

Needs $\dot{H} = \dot{M}_f \Delta T_f c_f$

- **Fluid availability**
  - Native or introduced
  - H_2O/CO_2 working fluids?
- **Fluid transmission**
  - Permeability microD to mD?
  - Distributed permeability
- **Thermal efficiency**
  - Large heat transfer area
  - Small conduction length
- **Long-lived**
  - Maintain mD and HT-area
  - Chemistry
- **Environment**
  - Induced seismicity
  - Fugitive fluids
- **Ubiquitous**

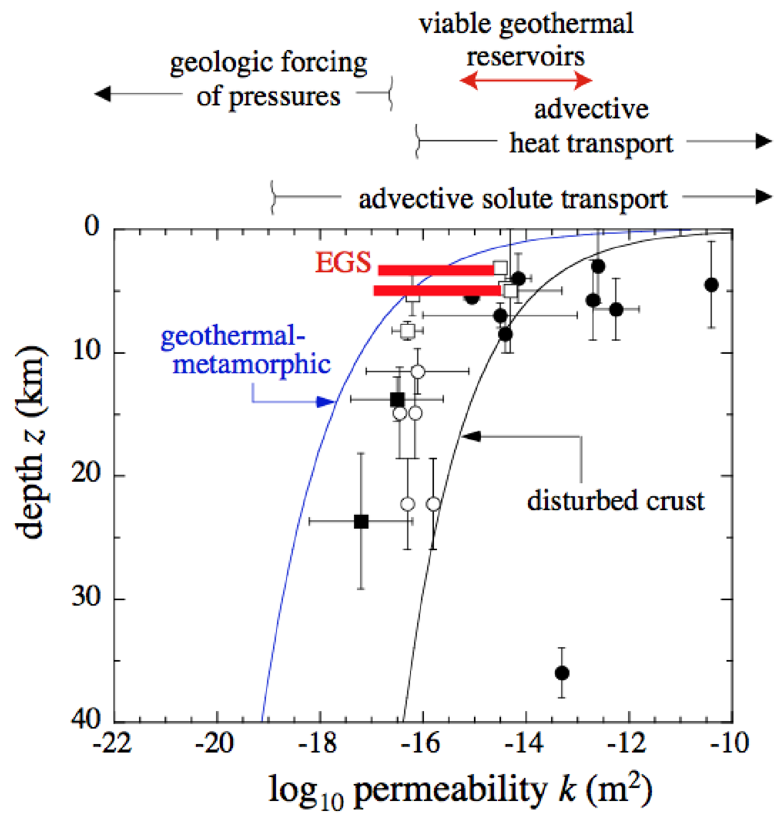

Figure 12: Evidence for relatively high crustal-scale permeabilities showing showing power-law fit to data. Geothermal-metamorphic curve is the best-fit to geothermal-metamorphic data [*Manga and Ingebritsen*, 1999, 2002]. "Disturbed-crust" curve interpolates midpoints in reported ranges in *k* and *z* for a given locality [*Manning and Ingebritsen*, 2010, their Table 1]; error bars depict the full permissible range for a plotted locality and are not Gaussian errors, and the Dobi (Afar) earthquake swarm is not shown on this plot (it is off-scale). Red lines indicate permeabilities before and after EGS reservoir stimulation at Soultz (upper line) and Basel (lower line) from *Evans et al.* [2005] and *Häring et al.* [2008], respectively. Arrows above the graph show the range of permeability in which different processes dominate.

Steve.ai [Ingebritsen and Manning, various, in Manga et al., 2012]

Thermal Drawdown SGRs -vs- EGS

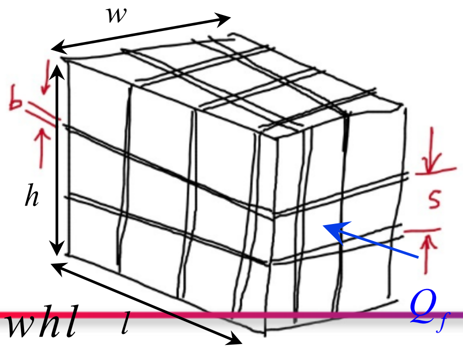

$V = volume = whl$

$$\dot{H}_{solid} \sim A\lambda_R \frac{dT}{dx} \sim \frac{V\lambda_R \Delta T}{s^2}$$

$$\dot{H}_{fluid} \sim Q_f \rho_W c_W \Delta T$$

$$\frac{\dot{H}_f}{\dot{H}_s} \sim \frac{\rho_W c_W}{\lambda_R} \frac{Q_f s^2}{V} = Q_D$$

In-Reservoir Water Temperature Distributions:

$SGRs:$

$\dot{H}_s \rightarrow 0$

$\dot{H}_f / \dot{H}_s \rightarrow 0$

$Q_D \rightarrow 0$

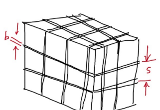

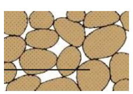

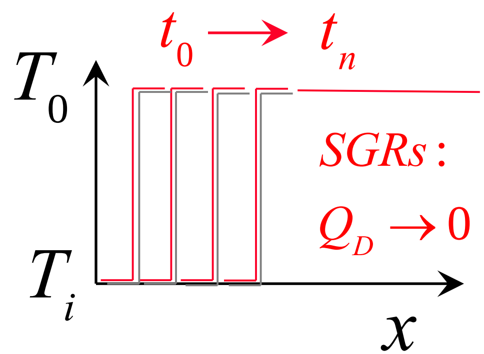

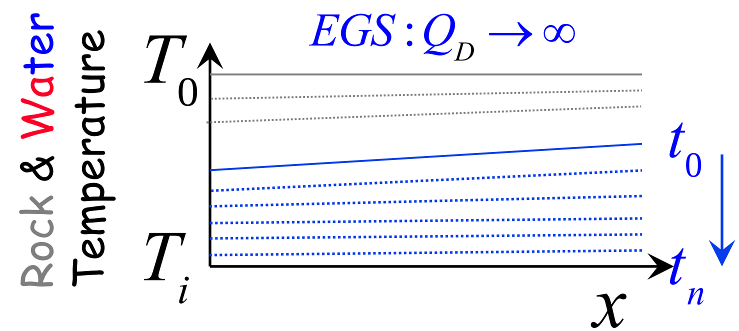

$EGS:$

$\dot{H}_f \rightarrow \infty$

$\dot{H}_f / \dot{H}_s \rightarrow \infty$

$Q_D \rightarrow \infty$

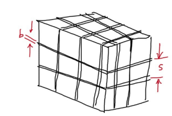

Thermal Output:

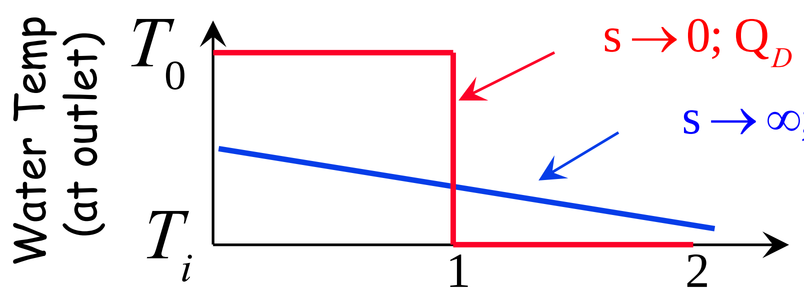

$s \rightarrow 0$; $Q_D \rightarrow 0$; Thermal-front present

$s \rightarrow \infty$; $Q_D \rightarrow \infty$; Thermal front absent

$$t_D = \frac{r_W c_W}{r_R c_R} \frac{Q_f t}{V}$$

Thermal Recovery at Field Scale

Parallel Flow Model

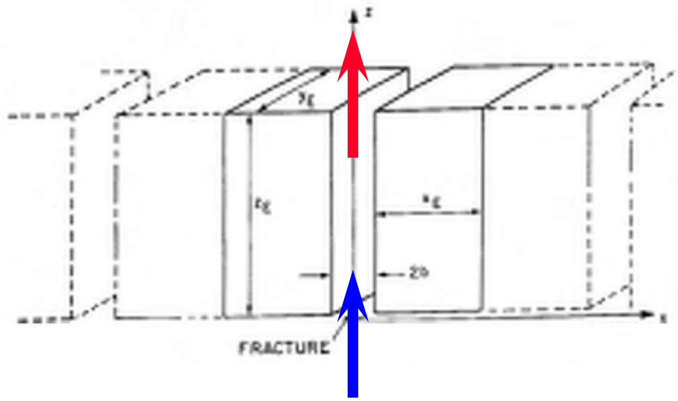

[Gringarten and Witherspoon, Geothermics,1974]

Spherical Reservoir Model

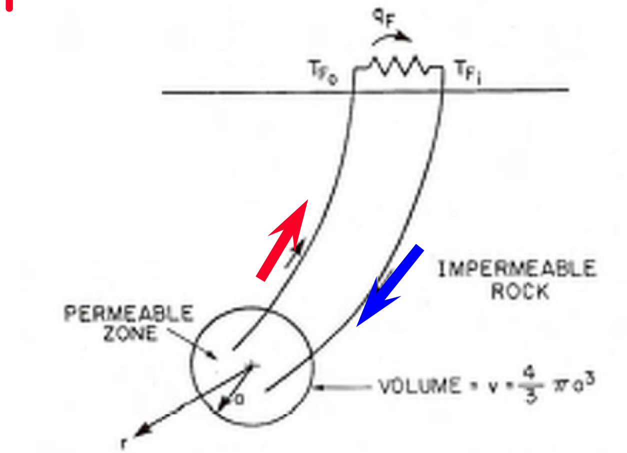

[Elsworth, JGR, 1989]

Dimensionless temperature

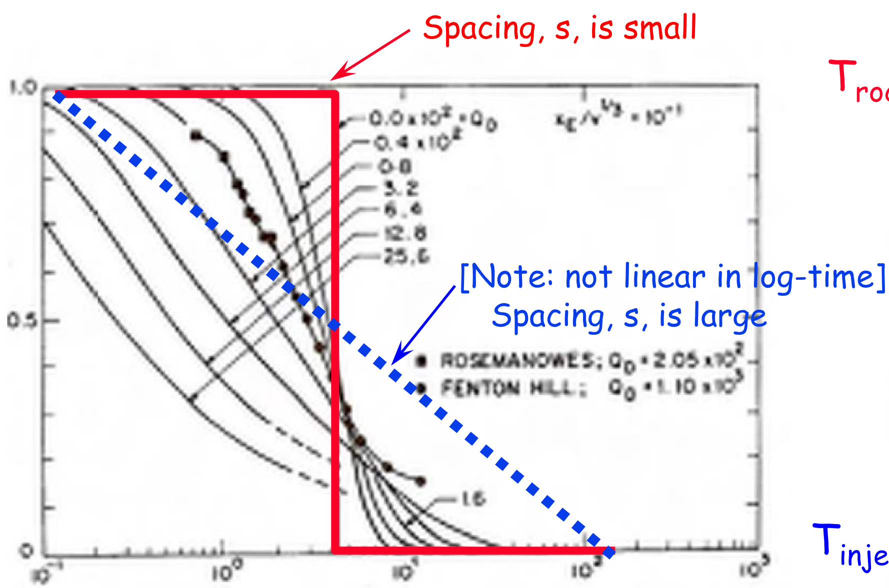

T_{rock}

$T_{injection}$

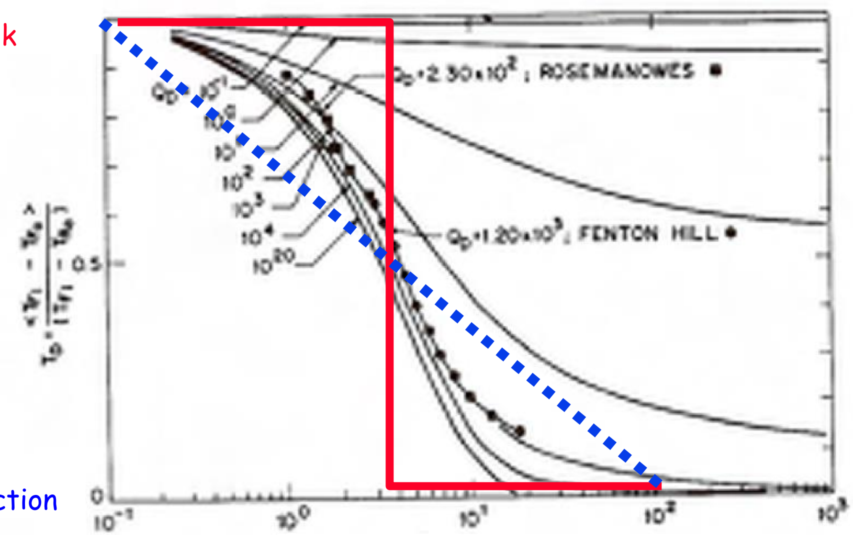

Dimensionless time

[Elsworth, JVGR, 1990]

Dimensionless time

Slow Earthquakes and the spectrum of fault slip behavior

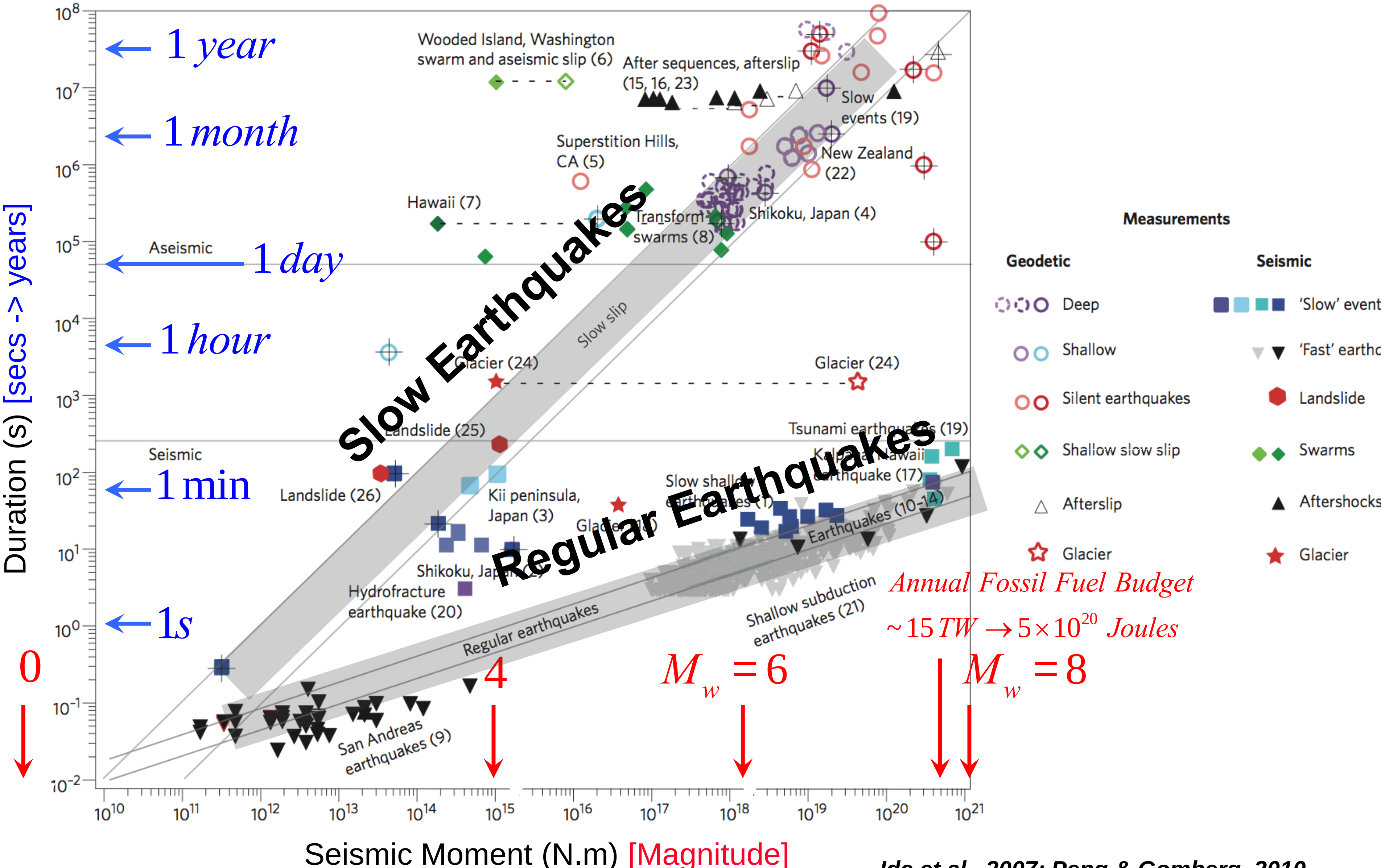

Ide et al., 2007; Peng & Gomberg, 2010

Approaches – Rate-State versus Brittle Behavior

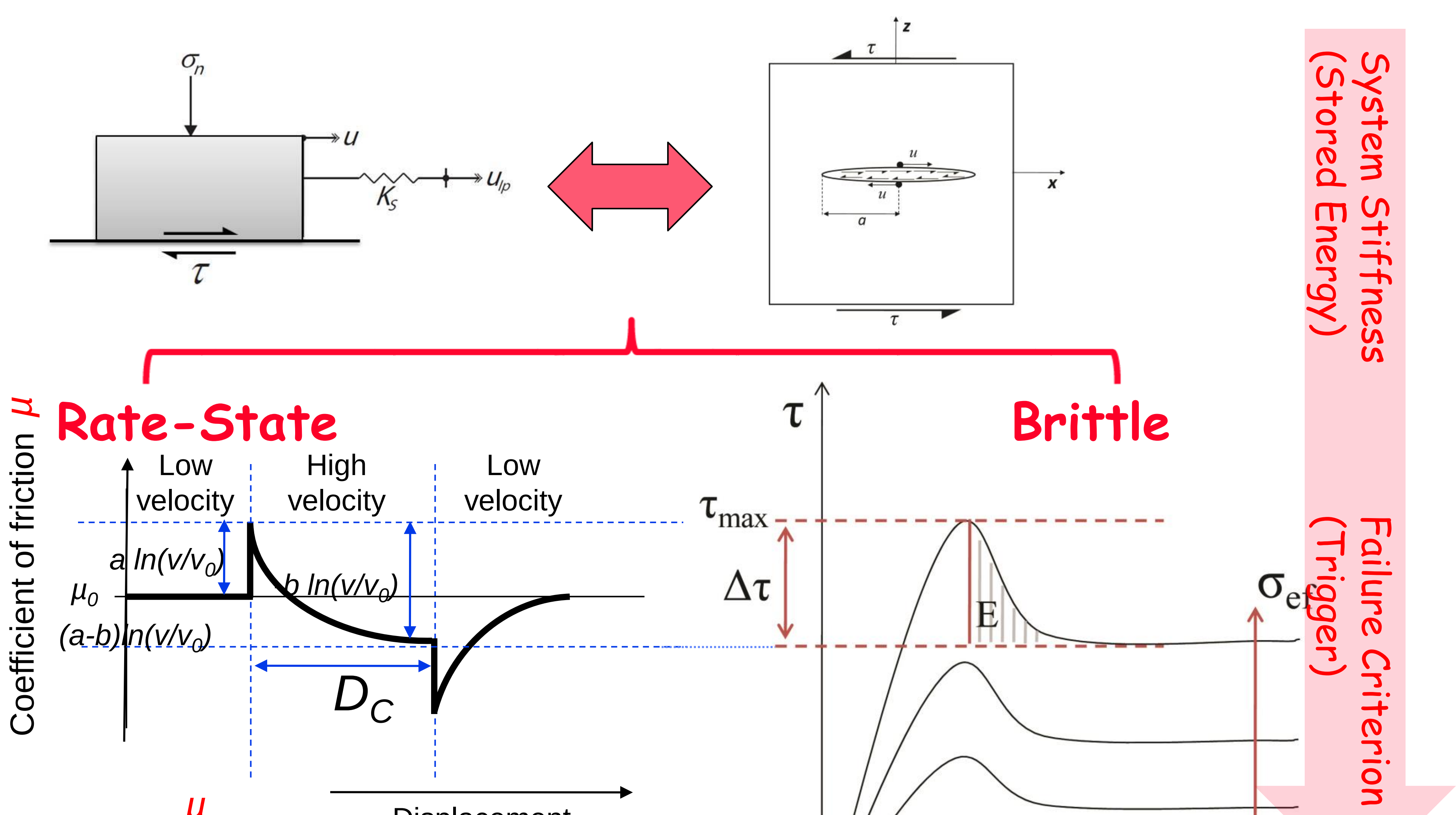

$$\tau = \left[\mu_0 + a \ln\left(\frac{v}{v_0}\right) + b \ln\left(\frac{v_0 \theta}{D_C}\right) \right] \sigma_{ef} .$$

g3.ems.psu.edu

Requirements for Instability

1. Shear strength on the fault is exceeded – *i.e.*

$$\tau > \mu \sigma'_n$$

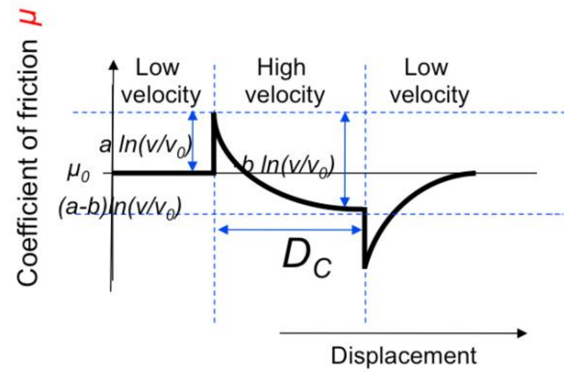

2. When failure occurs, strength is velocity (or strain) weakening - *i.e.*

$$a - b < 0$$

2. That the failure is capable of ejecting the stored strain energy adjacent to the fault (shear modulus and fault length) - *i.e.*

$$\frac{G}{l} < K_c = \frac{(b-a)\sigma_n'}{D_c}$$

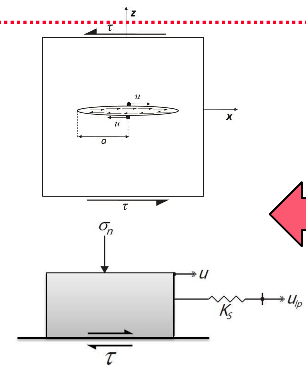

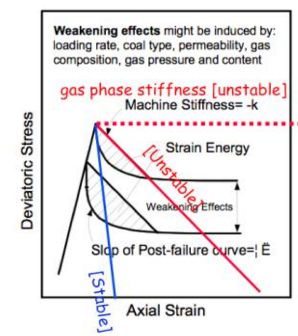

4. That effective normal stresses evolve that do not dilatantly harden the fault and arrest it via the failure criterion of #1 – *i.e.*

$$1 >> v_D = \frac{w^2}{k} \frac{v_s \eta}{K_s D_c}$$

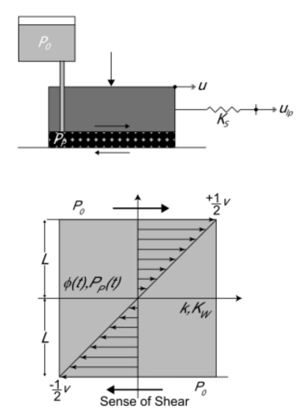

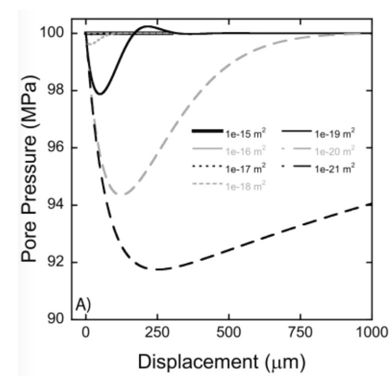

Anomalous Distribution of MEQs - Newberry

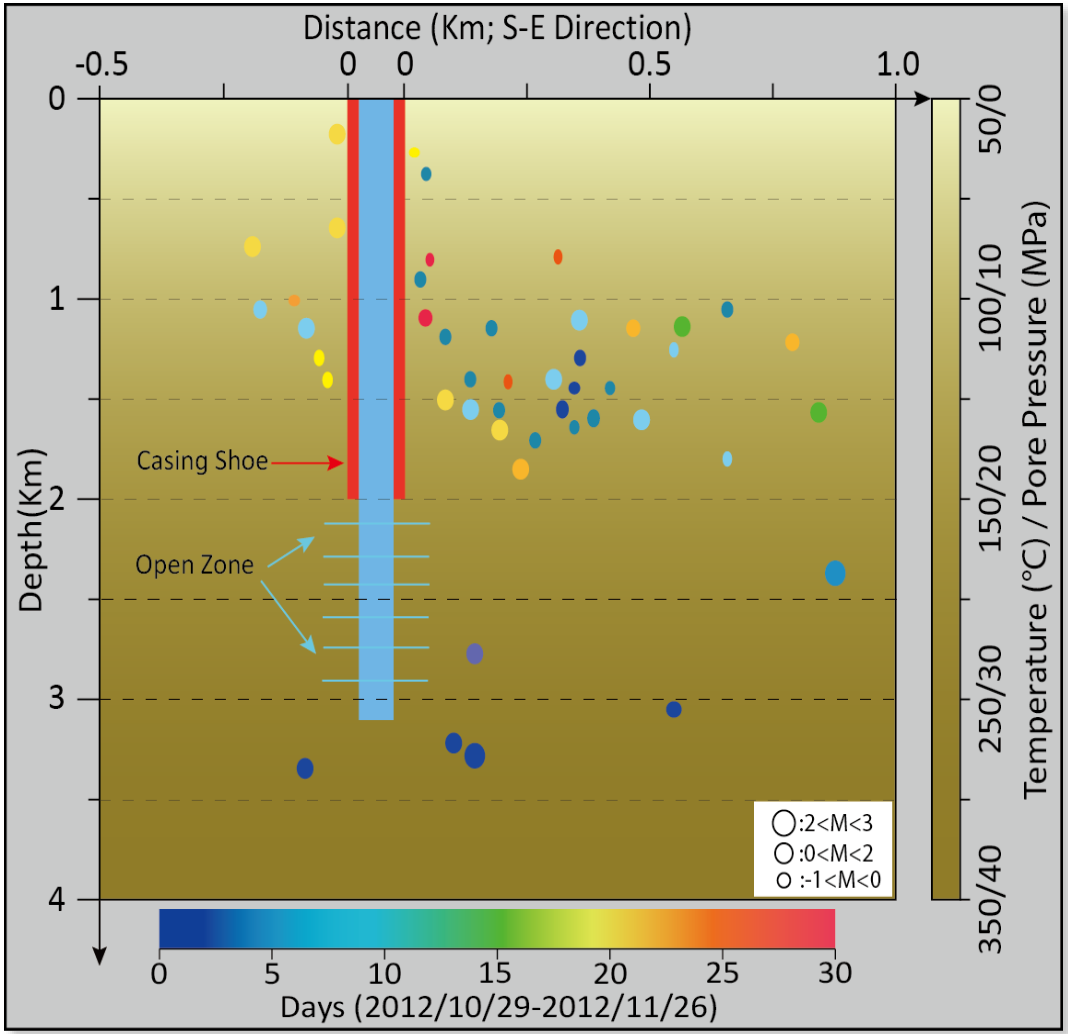

Wellbore Settings

- 0-2000m: Casing shoe
- 2000m-3000m: open zone

Spatial Anomaly

- Bimodal depth distribution
- Below 1950 m, only a few MEQs occurred.
- Between 500m and 1800m, 90% MEQs occurred adjacent to the cased part.

Temporal Anomaly

- Deep MEQs occurred within 4 days and diminished after that time.
- Shallow MEQs occurred since the 4^{th} day.

Questions:

- What is the mechanism of this anomalous distribution of MEQs?
- What can this anomalous distribution of MEQs imply?

RSF Key Controls – (a-b) and K_c

Velocity-Step Experiment:

a-b<0 suggests velocity weakening, unstable slip (i.e., seismic slip) will occur.

a-b>0 suggests velocity strengthening, stable sliding (i.e., aseismic slip) will occur.

Rate-State Response

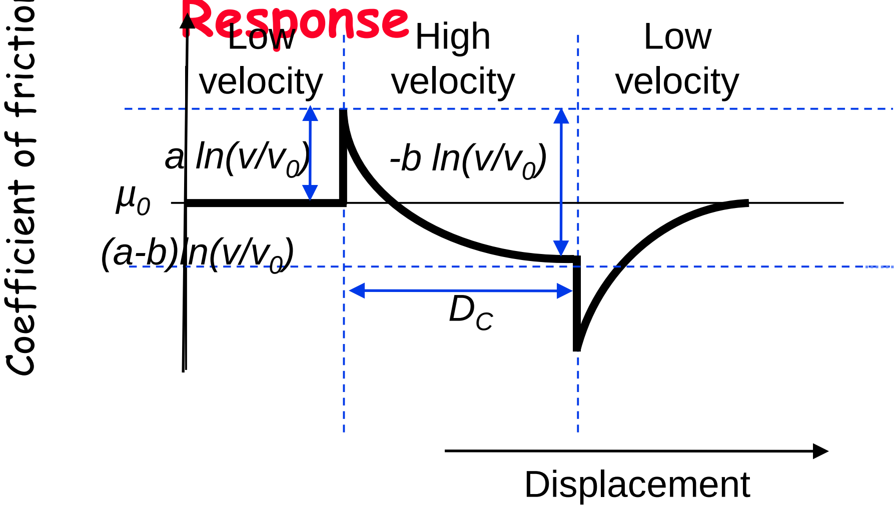

$$K_c = \frac{\sigma_n (b-a)}{D_c}$$

If $K < K_c$ suggests Frictional Instability

If $K > K_c$ suggests Frictional Stability

Dynamic friction varies with velocity.

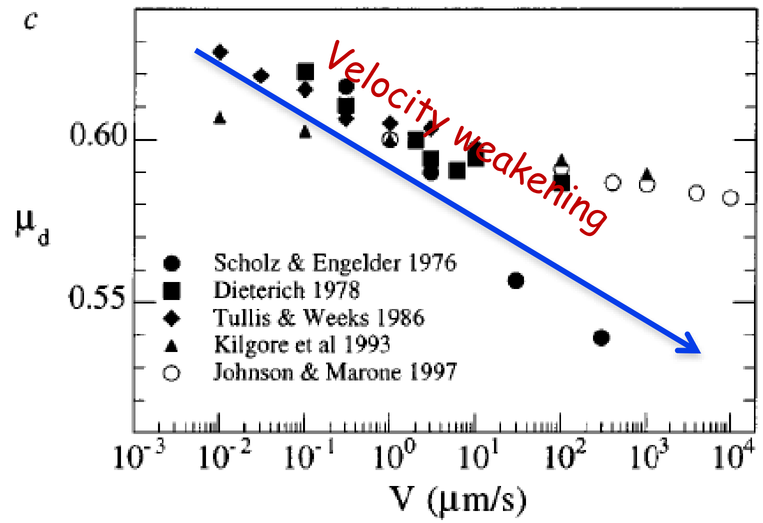

Static friction and healing vary with loading rate and hold time.

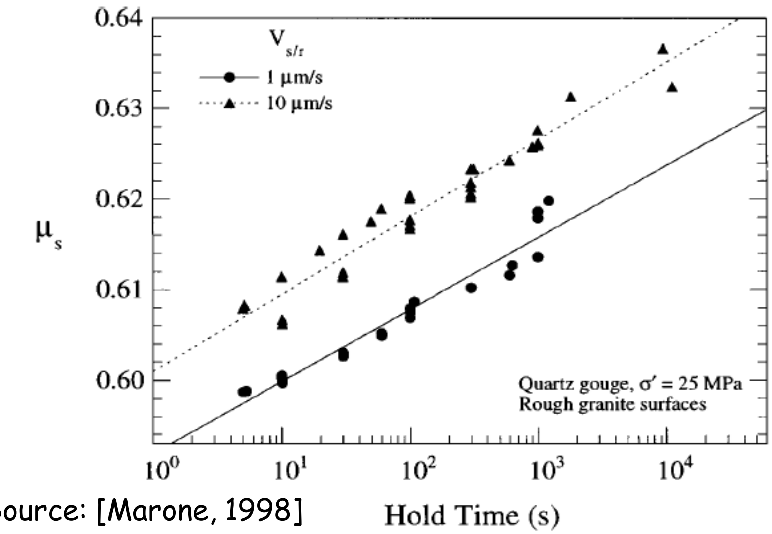

Source: [Marone, 1998]

RSF Properties

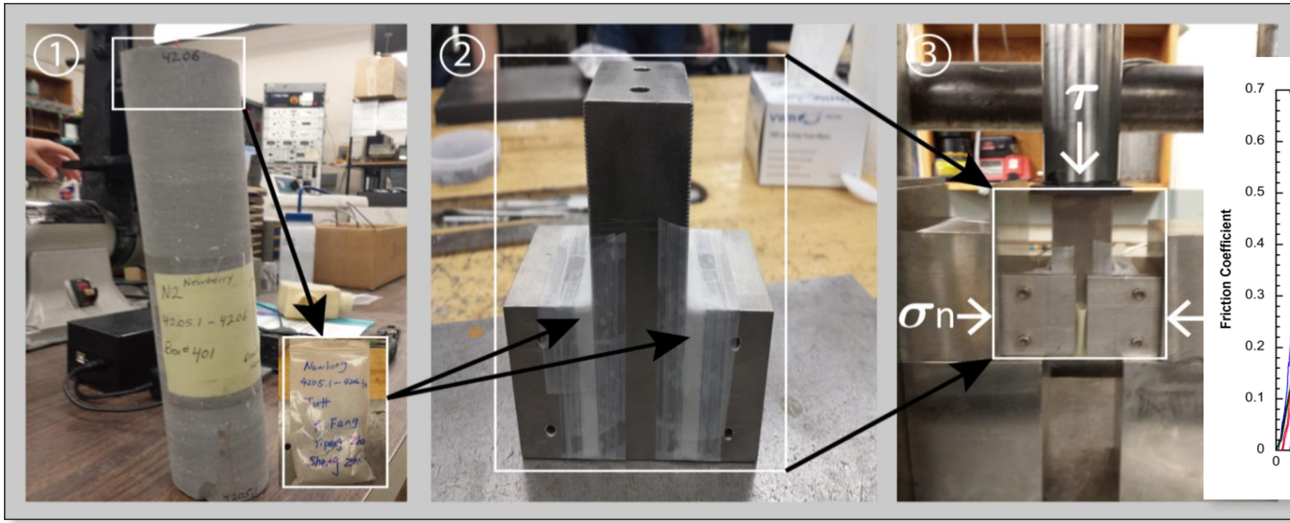

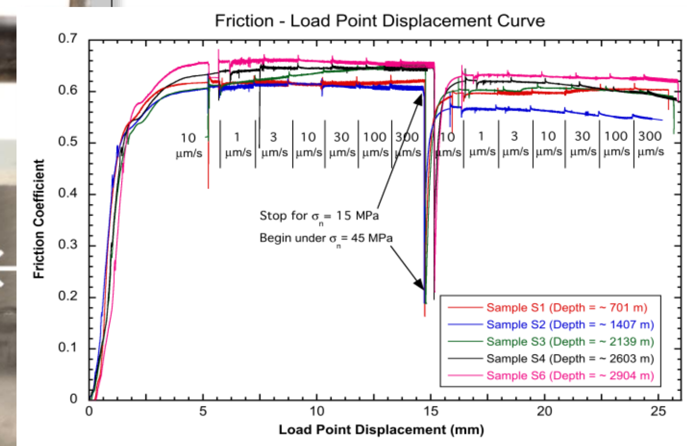

Preliminary RSF Properties

(a-b) at 15 MPa

(a-b) at 45 MPa

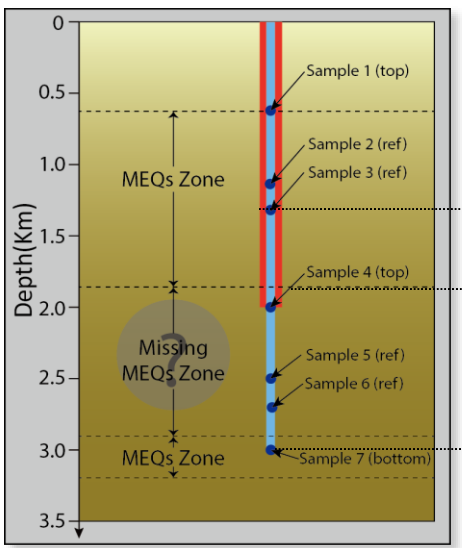

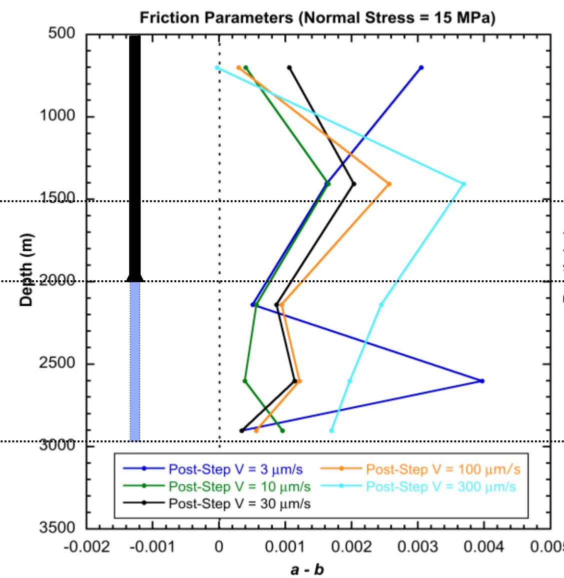

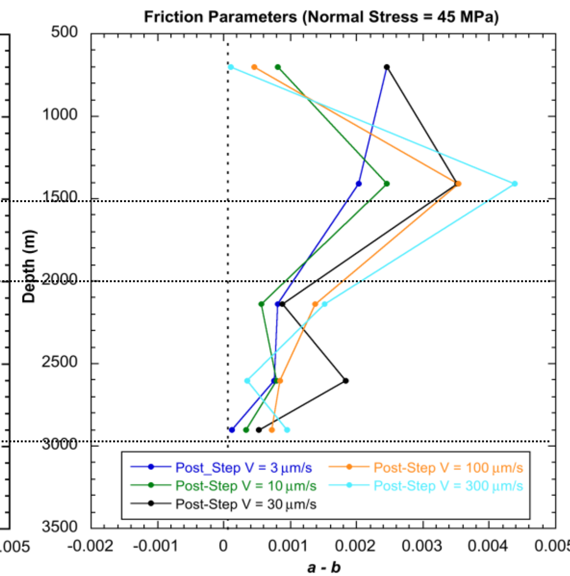

Conclusions

Complex THM and THC Interactions Influence Reservoir Evolution

- Permeability evolution is strongly influenced by these processes
- In some instances the full THMC quadruplet is important
- Effects are exacerbated by heterogeneity and anisotropy

Spatial and Temporal Evolution

- Physical controls (perm, thermal diffusion, kinetics) control progress
- Effects occur in order of fluid pressure (M), thermal dilation (TM), chemical alteration (C)
- Spatial halos also propagate in this same order of pressure, temperature, chemistry

Induced Seismicity

- Mechanisms that control permeability (i.e. HTC stress) also influence seismicity
- Event magnitudes controlled by stress-drop and fracture size
  - Also sharpness of thermal front – sharper front larger event?
    but moderated by patch size inside front
- Distribution controlled by fracture location and sizes (if no new fractures created)
- Timing controlled by:
  - Relative magnitude of stress change effects (pressure, temp, chem)
  - Rates of propagation and self-propagation of those stress-change fronts